secondary envelopment of murine cytomegalovirus. J. Virol. 85:9254–9267. http://dx.doi.org/10.1128/JVI.00443-11.
16. Meckes DG, Jr, Wills JW. 2007. Dynamic interactions of the UL16 tegument protein with the capsid of herpes simplex virus. J. Virol. 81:13028–13036. http://dx.doi.org/10.1128/JVI.01306-07.
17. Nalwanga D, Rempel S, Roizman B, Baines JD. 1996. The UL 16 gene product of herpes simplex virus 1 is a virion protein that colocalizes with intranuclear capsid proteins. Virology 226:236–242. http://dx.doi.org/10.1006/viro.1996.0651.
18. Oshima S, Daikoku T, Shibata S, Yamada H, Goshima F, Nishiyama Y. 1998. Characterization of the UL16 gene product of herpes simplex virus type 2. Arch. Virol. 143:863–880. http://dx.doi.org/10.1007/s007050050338.
19. Yeh PC, Meckes DG, Jr, Wills JW. 2008. Analysis of the interaction between the UL11 and UL16 tegument proteins of herpes simplex virus. J. Virol. 82:10693–10700. http://dx.doi.org/10.1128/JVI.01230-08.
20. Johnson DC, Baines JD. 2011. Herpesviruses remodel host membranes for virus egress. Nat. Rev. Microbiol. 9:382–394. http://dx.doi.org/10.1038/nrmicro2559.
21. Baines JD, Roizman B. 1991. The open reading frames UL3, UL4, UL10, and UL16 are dispensable for the replication of herpes simplex virus 1 in cell culture. J. Virol. 65:938–944.
22. Dunn W, Chou C, Li H, Hai R, Patterson D, Stolc V, Zhu H, Liu F. 2003. Functional profiling of a human cytomegalovirus genome. Proc. Natl. Acad. Sci. U. S. A. 100:14223–14228. http://dx.doi.org/10.1073/pnas.2334032100.
23. Klupp BG, Bottcher S, Granzow H, Kopp M, Mettenleiter TC. 2005. Complex formation between the UL16 and UL21 tegument proteins of pseudorabies virus. J. Virol. 79:1510–1522. http://dx.doi.org/10.1128/JVI.79.3.1510-1522.2005.
24. Phillips SL, Bresnahan WA. 2012. The human cytomegalovirus (HCMV) tegument protein UL94 is essential for secondary envelopment of HCMV virions. J. Virol. 86:2523–2532. http://dx.doi.org/10.1128/JVI.06548-11.
25. Yu D, Silva MC, Shenk T. 2003. Functional map of human cytomegalovirus AD169 defined by global mutational analysis. Proc. Natl. Acad. Sci. U. S. A. 100:12396–12401. http://dx.doi.org/10.1073/pnas.1635160100.
26. Chadha P, Han J, Starkey JL, Wills JW. 2012. Regulated interaction of tegument proteins UL16 and UL11 from herpes simplex virus. J. Virol. 86:11886–11898. http://dx.doi.org/10.1128/JVI.01879-12.
27. Phillips SL, Cygnar D, Thomas A, Bresnahan WA. 2012. Interaction between the human cytomegalovirus tegument proteins UL94 and UL99 is essential for virus replication. J. Virol. 86:9995–10005. http://dx.doi.org/10.1128/JVI.01078-12.
28. Stellberger T, Hauser R, Baiker A, Pothineni VR, Haas J, Uetz P. 2010. Improving the yeast two-hybrid system with permutated fusions proteins: the varicella zoster virus interactome. Proteome Sci. 8:8. http://dx.doi.org/10.1186/1477-5956-8-8.
29. Uetz P, Dong YA, Zeretzke C, Atzler C, Baiker A, Berger B, Rajagopala SV, Roupelieva M, Rose D, Fossum E, Haas J. 2006. Herpesviral protein networks and their interaction with the human proteome. Science 311:239–242. http://dx.doi.org/10.1126/science.1116804.
30. Sadaoka T, Yanagi T, Yamanishi K, Mori Y. 2010. Characterization of the varicella-zoster virus ORF50 gene, which encodes glycoprotein M. J. Virol. 84:3488–3502. http://dx.doi.org/10.1128/JVI.01838-09.
31. Niwa H, Yamamura K, Miyazaki J. 1991. Efficient selection for high-expression transfectants with a novel eukaryotic vector. Gene 108:193–199. http://dx.doi.org/10.1016/0378-1119(91)90434-D.
32. Sadaoka T, Yamanishi K, Mori Y. 2006. Human herpesvirus 7 U47 gene products are glycoproteins expressed in virions and associate with glycoprotein H. J. Gen. Virol. 87:501–508. http://dx.doi.org/10.1099/vir.0.81374-0.
33. Okuno T, Yamanishi K, Shiraki K, Takahashi M. 1983. Synthesis and processing of glycoproteins of varicella-zoster virus (VZV) as studied with monoclonal antibodies to VZV antigens. Virology 129:357–368. http://dx.doi.org/10.1016/0042-6822(83)90175-7.
34. Nagaike K, Mori Y, Gomi Y, Yoshii H, Takahashi M, Wagner M, Koszinowski U, Yamanishi K. 2004. Cloning of the varicella-zoster virus genome as an infectious bacterial artificial chromosome in Escherichia coli. Vaccine 22:4069–4074. http://dx.doi.org/10.1016/j.vaccine.2004.03.062.
35. Narayanan K, Williamson R, Zhang Y, Stewart AF, Ioannou PA. 1999. Efficient and precise engineering of a 200 kb beta-globin human/bacterial artificial chromosome in E. coli DH10B using an inducible homologous recombination system. Gene Ther. 6:442–447. http://dx.doi.org/10.1038/sj.gt.3300901.
36. Cherepanov PP, Wackernagel W. 1995. Gene disruption in Escherichia coli: TcR and KmR cassettes with the option of Flp-catalyzed excision of the antibiotic-resistance determinant. Gene 158:9–14. http://dx.doi.org/10.1016/0378-1119(95)00193-A.
37. Hobom U, Brune W, Messerle M, Hahn G, Koszinowski UH. 2000. Fast screening procedures for random transposon libraries of cloned herpesvirus genomes: mutational analysis of human cytomegalovirus envelope glycoprotein genes. J. Virol. 74:7720–7729. http://dx.doi.org/10.1128/JVI.74.17.7720-7729.2000.
38. Shevchenko A, Wilm M, Vorm O, Mann M. 1996. Mass spectrometric sequencing of proteins silver-stained polyacrylamide gels. Anal. Chem. 68:850–858. http://dx.doi.org/10.1021/ac950914h.
39. Carpenter JE, Henderson EP, Grose C. 2009. Enumeration of an extremely high particle-to-PFU ratio for varicella-zoster virus. J. Virol. 83:6917–6921. http://dx.doi.org/10.1128/JVI.00081-09.
40. Shiraki K, Takahashi M. 1982. Virus particles and glycoprotein excreted from cultured cells infected with varicella-zoster virus (VZV). J. Gen. Virol. 61:271–275. http://dx.doi.org/10.1099/0022-1317-61-2-271.
41. Gabel CA, Dubey L, Steinberg SP, Sherman D, Gershon MD, Gershon AA. 1989. Varicella-zoster virus glycoprotein oligosaccharides are phosphorylated during posttranslational maturation. J. Virol. 63:4264–4276.
42. Gershon AA, Sherman DL, Zhu Z, Gabel CA, Ambron RT, Gershon MD. 1994. Intracellular transport of newly synthesized varicella-zoster virus: final envelopment in the trans-Golgi network. J. Virol. 68:6372–6390.
43. Harson R, Grose C. 1995. Egress of varicella-zoster virus from the melanoma cell: a tropism for the melanocyte. J. Virol. 69:4994–5010.
44. Ali MA, Li Q, Fischer ER, Cohen JI. 2009. The insulin degrading enzyme binding domain of varicella-zoster virus (VZV) glycoprotein E is important for cell-to-cell spread and VZV infectivity, while a glycoprotein I binding domain is essential for infection. Virology 386:270–279. http://dx.doi.org/10.1016/j.virol.2009.01.023.
45. Tischer BK, Kaufer BB, Sommer M, Wussow F, Arvin AM, Osterrieder N. 2007. A self-excisable infectious bacterial artificial chromosome clone of varicella-zoster virus allows analysis of the essential tegument protein encoded by ORF9. J. Virol. 81:13200–13208. http://dx.doi.org/10.1128/JVI.01148-07.
46. Yamagishi Y, Sadaoka T, Yoshii H, Somboonthum P, Imazawa T, Nagaike K, Ozono K, Yamanishi K, Mori Y. 2008. Varicella-zoster virus glycoprotein M homolog is glycosylated, is expressed on the viral envelope, and functions in virus cell-to-cell spread. J. Virol. 82:795–804. http://dx.doi.org/10.1128/JVI.01722-07.
47. Betts MJ, Russell RB. 22 May 2003. Amino acid properties and consequences of substitutions. Chapter 14. *In* Barnes MR, Gray IC (ed), Bioinformatics for geneticists. Wiley, Chichester, West Sussex, England. http://dx.doi.org/10.1002/0470867302.ch14.
48. Burley SK, Petsko GA. 1985. Aromatic-aromatic interaction: a mechanism of protein structure stabilization. Science 229:23–28. http://dx.doi.org/10.1126/science.3892686.
49. Eidenschink LA, Kier BL, Andersen NH. 2009. Determinants of fold stabilizing aromatic-aromatic interactions in short peptides. Adv. Exp. Med. Biol. 611:73–74. http://dx.doi.org/10.1007/978-0-387-73657-0_32.
50. Meckes DG, Jr, Marsh JA, Wills JW. 2010. Complex mechanisms for the packaging of the UL16 tegument protein into herpes simplex virus. Virology 398:208–213. http://dx.doi.org/10.1016/j.virol.2009.12.004.
51. Han J, Chadha P, Meckes DG, Jr, Baird NL, Wills JW. 2011. Interaction and interdependent packaging of tegument protein UL11 and glycoprotein E of herpes simplex virus. J. Virol. 85:9437–9446. http://dx.doi.org/10.1128/JVI.05207-11.
52. Harper AL, Meckes DG, Jr, Marsh JA, Ward MD, Yeh PC, Baird NL, Wilson CB, Semmes OJ, Wills JW. 2010. Interaction domains of the UL16 and UL21 tegument proteins of herpes simplex virus. J. Virol. 84:2963–2971. http://dx.doi.org/10.1128/JVI.02015-09.

Downloaded from http://jvi.asm.org/ on December 18, 2013 by KUBE UNIVERSITY

PLOS ONE

Karyopherin Alpha2 Is Essential for rRNA Transcription and Protein Synthesis in Proliferative Keratinocytes

Noriko Umegaki-Arao[1], Katsuto Tamai[2]*, Keisuke Nimura[3], Satoshi Serada[4], Tetsuji Naka[4], Hajime Nakano[5], Ichiro Katayama[1]

1 Department of Dermatology, Osaka University Graduate School of Medicine, Osaka, Japan, **2** Department of Stem Cell Therapy Science, Osaka University Graduate School of Medicine, Osaka, Japan, **3** Division of Gene Therapy Science, Osaka University Graduate School of Medicine, Osaka, Japan, **4** National Institute of Biomedical Innovation Laboratory for Immune Signal, Osaka, Japan, **5** Department of Dermatology, Hirosaki University School of Medicine, Hirosaki, Japan

Abstract

Karyopherin proteins mediate nucleocytoplasmic trafficking and are critical for protein and RNA subcellular localization. Recent studies suggest KPNA2 expression is induced in tumor cells and is strongly associated with prognosis, although the precise roles and mechanisms of KPNA2 overexpression in proliferative disorders have not been defined. We found that KPNA2 expression is induced in various proliferative disorders of the skin such as psoriasis, Bowen's disease, actinic keratosis, squamous cell carcinoma, Paget's disease, Merkel cell carcinoma, and mycosis fungoides. siRNA-mediated KPNA suppression revealed that KPNA2 is essential for significant suppression of HaCaT proliferation under starvation conditions. Ribosomal RNA transcription and protein synthesis were suppressed by starvation combined with knockdown of KPNA (including KPNA2) expression. KPNA2 localized to the nucleolus and interacted with proteins associated with mRNA processing, ribonucleoprotein complex biogenesis, chromatin modification, and transcription, as demonstrated by tandem affinity purification and mass spectrometry. KPNA2 may be an important promoter of ribosomal RNA and protein synthesis in tumor cells.

Citation: Umegaki-Arao N, Tamai K, Nimura K, Serada S, Naka T, et al. (2013) Karyopherin Alpha2 Is Essential for rRNA Transcription and Protein Synthesis in Proliferative Keratinocytes. PLoS ONE 8(10): e76416. doi:10.1371/journal.pone.0076416

Editor: Andrzej T. Slominski, University of Tennessee, United States of America

Received November 9, 2012; **Accepted** August 29, 2013; **Published** October 3, 2013

Copyright: © 2013 Umegaki-Arao et al. This is an open-access article distributed under the terms of the Creative Commons Attribution License, which permits unrestricted use, distribution, and reproduction in any medium, provided the original author and source are credited.

Funding: This work was supported by a Grant-in-Aid of Scientific Research from the Ministry of Education, Culture, Science and Technology of Japan, and a Health and Labour Science Research Grant from the Ministry of Health, Labour and Welfare of Japan. The funders had no role in study design, data collection and analysis, decision to publish, or preparation of the manuscript.

Competing Interests: The authors have declared that no competing interests exist.

* E-mail: tamai@gts.med.osaka-u.ac.jp

Introduction

Recent studies have defined the molecular mechanisms of nucleocytoplasmic signal transduction by karyopherins (KPNs), which function as receptors for various intracellular molecules and mediate nuclear import and export during interphase. In humans, the karyopherin alpha (KPNA) family consists of at least 7 family members, all of which interact with karyopherin beta (KPNB) 1 and transport various proteins and RNAs through the nuclear pores in an energy-dependent manner [1–3]. Various extracellular environmental changes activate intracellular signaling cascades by which cells exchange activated signaling molecules between the nucleus and cytoplasm via the KPN-mediated machinery to regulate proliferation and differentiation status [2,4–6]. KPNA2 expression in human epidermal keratinocytes, but not in human dermal fibroblasts, is differentially regulated by transforming growth factor (TGF)-β_1 and interferon (IFN)-γ, both of which are established modulators of epidermal proliferation and differentiation [4]. KPNA2 also mediates the translocation of epidermal differentiation-inducing signals into the nucleus by recruiting transcription factors such as interferon regulatory factor-1 (IRF-1), thereby inducing IFN-γ-mediated epidermal differentiation [4]. Karyopherin alphas also mediate mitotic spindle assembly [7–9] and nuclear membrane formation [10]. KPNB1 is also a global regulator of mitotic spindle assembly, centrosome dynamics, nuclear membrane formation, and nuclear pore complex assembly [11,12]. Recent studies have revealed that KPNs including KPNA2 are overexpressed in various kinds of tumors such as breast cancer, cervical cancer, non-small cell lung cancer, prostate cancer, and primary cutaneous melanoma, and that expression levels in these tumors are closely associated with prognosis [13–18]. Nevertheless, the precise roles and mechanisms of KPN overexpression in proliferative disorders have not been defined.

The rate of cell growth and proliferation is proportional to the rate of protein synthesis, which is tightly linked to ribosome biologics [19,20]. RNA synthesis and ribosome construction occur in the nucleolus and their control is important for regulating protein synthesis; however, the precise mechanisms and roles of karyopherins in regulating rRNA and protein synthesis remain unclear.

We report KPNA2 induction in proliferation disorders regardless of malignancy, and suggest KPNA2 regulates rRNA transcription and general protein synthesis in the nucleolus to maintain proliferation.

Materials and Methods

Skin Samples

Written informed consent was obtained from all patients, and the study protocol was approved by Medical Ethics Committee of Osaka University.

Cell Culture

HaCaT cells, an immortalized, nontumorigenic keratinocyte cell line, were cultured in Dulbecco's modified Eagle's medium (DMEM; Nacalai Tesque) containing 10% fetal bovine serum (FBS) at 37°C under 5% CO_2-95% air.

RNA Purification and Reverse Transcription-quantitative Polymerase Chain Reaction

Total RNA was isolated from HaCaT cells with an RNA isolation kit (Qiagen) and reverse transcribed with SuperScript III reverse transcriptase (Invitrogen). Expression of pre-rRNA was determined by using Power SYBR green PCR Master Mix (Applied Biosystems) according to the manufacturer's protocol. β-Actin was used to normalize target gene expression. PCR amplification was performed with 5′-ATCGTCCACCGCAAATGCTTCTA-3′ and 5′-AGCCATGCCAATCTCATCTTGTT-3′ for β-actin and 5′-GAACGGTGGTGTGTCGTTC-3′ and 5′-GCGTCTCGTCTCGTCTCACT-3′ for pre-rRNA [21]. PCR cycling conditions were 40 cycles of denaturing at 92°C for 15 sec and annealing at 60°C for 60 sec on an ABI Prism 7000 sequence detection system (Applied Biosystems).

Small Interfering RNA and Plasmid DNA Transfection

Small interfering RNAs (siRNAs) specific for KPNA1, 2, 3, and 4 and the control stealth siRNA were obtained from Invitrogen. Cells (1.5×10^6) were transfected with 100 ng siRNAs mixture using the Neon transfection system (Invitrogen). We performed the knockdown studies with each siRNA, which ensured more than 50–70% suppression of KPNA2 mRNA and protein.

MTS

[3-(4,5-dimethylthiazol-2-yl)-5(3-carboxymethoxyphenyl)-2-(4-sulfophenyl)-2H-tetrazolium] assay. HaCaT cells induced with each siRNA were seeded at their optimal cell density (7×10^4 cells/well) in 96-well microtiter plates and incubated to allow cell attachment. After 6 h, cells were incubated with 0.1% FBS DMEM for 24, 48, 72, and 120 h. At the end of each incubation period, cell viability was determined by using the CellTiter 96® AQ_{ueous} Non-Radioactive Cell Proliferation Assay (Promega) according to the manufacturer's instructions. Samples were incubated at 37°C in a humidified 5% CO_2 atmosphere for 1 h. Absorbance was measured at 490 nm using a microplate reader.

Immunohistochemistry

Slides of skin biopsies in paraffin blocks were stained with hematoxylin and eosin (HE) and anti-human KPNA2 mouse monoclonal antibody (BD Biosciences) (1:1000).

Immunofluorescence

HaCaT cells were fixed in 4% formaldehyde in phosphate-buffered saline (PBS) for 40 min. After rinsing twice with PBS, the cells were permeabilized in 0.5% Triton X-100 in PBS for 60 s and blocked with 2% skim milk overnight at 4°C. The cells were incubated with anti-UBF (Santa Cruz) and anti-KPNA2 antibodies for 1 h and stained with Alexa Fluor 546 goat anti-rabbit IgG and Alexa Fluor 488 goat anti-mouse IgG secondary antibodies (1:1000; Invitrogen A-11035 and A-11029) for 1 h. After washing with PBS, cells were counterstained with 0.5 mg/mL 4′, 6′-diamidino-2-phenylindole (DAPI) and mounted with Vectashield mounting medium (Vector Laboratories). Cells were analyzed using a Radiance 2100 confocal scanning-laser microscope (Bio-Rad) equipped with an Eclipse TE-2000 inverted microscope (Nikon) or a Nikon A1 confocal scanning-laser microscope equipped with a Nikon Eclipse Ti inverted microscope.

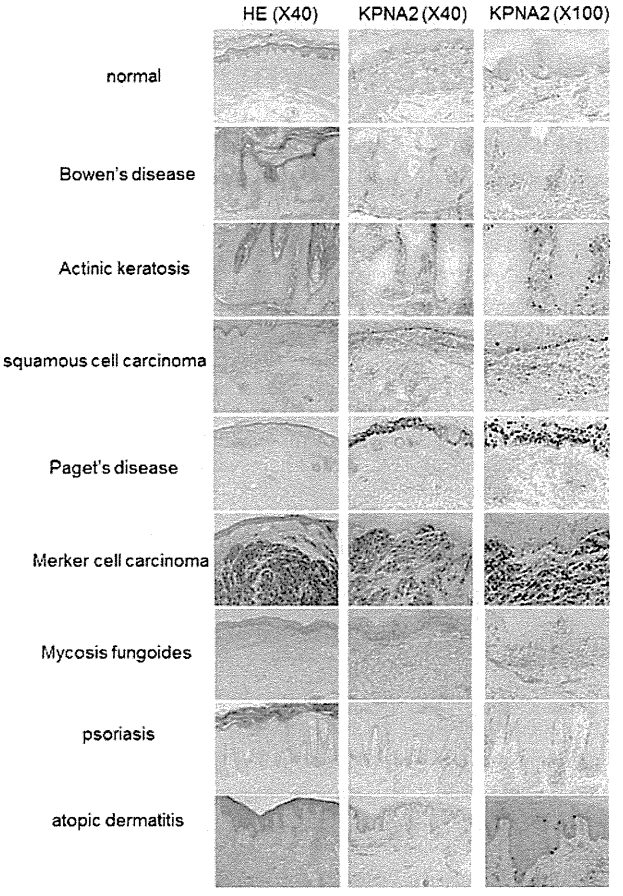

Figure 1. Overexpression of KPNA2 in proliferating cells. Immunohistochemistry showed KPNA2 was uniformly expressed throughout the epidermis in healthy skin, although KPNA2 overexpression was observed in the basal layer in psoriasis. In contrast, very few cells exhibited KPNA2 staining in the basal cells of atopic dermatitis. KPNA2 overexpression was observed in the tumor cells of Bowen's disease, actinic keratosis, squamous cell carcinoma, Paget's disease, Merkel cell carcinoma, and mycosis fungoides.
doi:10.1371/journal.pone.0076416.g001

Tandem Affinity Purification (TAP) and Mass Spectrometry

KPNA2 and GFP cDNAs were introduced into pCAGIP-gw-TAP by using Gateway technology (Invitrogen). KPNA2-TAP and GFP-TAP complexes were purified from HaCaT cell extracts using TAP technology [22,23]. Proteins were separated by SDS-PAGE and stained with the Silver Stain MS Kit (Wako Pure Chemical Industries). Protein bands were excised from the gel and digested with trypsin (Promega) [24]. NanoLC-MS/MS analyses were performed on a LTQ-Orbitrap XL mass spectrometer (Thermo Fisher Scientific) equipped with a nano-ESI source (AMR) and coupled to a Paradigm MG4 pump (Michrom Bioresources) and an autosampler (HTC PAL, CTC Analytics). A spray voltage of 1800 V was applied. The peptide mixture was separated on a MagicC18AQ column (100 μm×150 mm, 3.0 μm particle size, 300 Å, Michrom Bioresources) with a flow rate of 500 nl/min. A linear gradient of 5% to 45% B in 30 min, 45% to 95% B in 0.1 min, and 95% B for 2 min and 5% B was employed

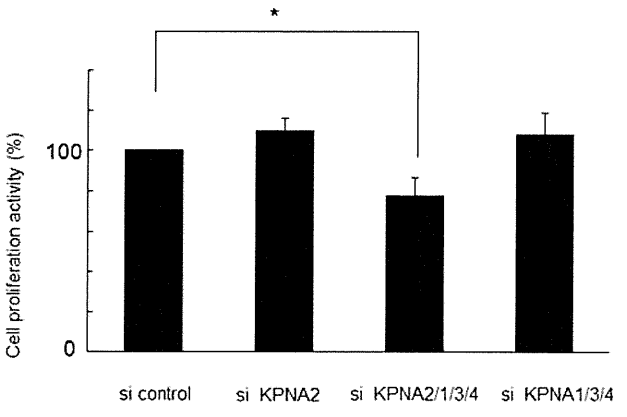

Figure 2. Suppression of cell growth by combined KPNA knockdown. Under starvation conditions (0.1% FBS), siRNA-mediated knockdown of KPNA2, 1, 3, and 4 suppressed cell growth after 120 h (*$p<0.05$). Only KPNA2 siRNA subtraction produced no change in proliferation.
doi:10.1371/journal.pone.0076416.g002

(A = 0.1% formic acid in 2% acetonitrile, B = 0.1% formic acid in 90% acetonitrile). Intact peptides were detected in the Orbitrap at 60,000 resolutions. For LC-MS/MS analysis, 6 precursor ions were selected for MS/MS scans in a data-dependent acquisition mode following each full scan (m/z, 350–1500). A lock mass function was used for the LTQ-Orbitrap to obtain constant mass accuracy during gradient analysis.

Peptides and proteins were identified by automated database searching the Swiss-Prot protein database (version 57.14x) with the MASCOT search program (version 1.0; Matrix Science) and a precursor mass tolerance of 10 p.p.m., a fragment ion mass tolerance of 0.8 Da, and strict trypsin specificity, allowing for up to 2 missed cleavages. Carbamidomethylation of cysteine was set as a fixed modification and oxidation of methionines was allowed as a variable modification.

Metabolic Labeling

HaCaT cells were labeled for 2 h with 100 mCi ^{35}S-methionine in methionine-free DMEM (Gibco) supplemented with 10% dialyzed serum. Protein was extracted with TNE buffer containing 50 mM Tris-HCl at pH 7.4, 150 mM NaCl, 2 mM EDTA, and 0.5% NP-40, then resuspended in 1% sodium dodecyl sulfate and boiled for 10 min at 100°C. Radioactivity was measured with a Beckmann Coulter liquid scintillation counter and normalized to protein content.

Transient Transfection and Luciferase Assay

The human pre-rRNA-luc vector was kindly provided by Dr. Samson Jacob [25]. HaCaT cells induced with each siRNA were seeded in a 12-well plate and transfected with 0.34 μg human-pre-rRNA-luc plasmid and Fugene 6 transfection reagent (Roche). The luciferase reporter assay was performed using a commercial luciferase assay kit (Promega). Data were normalized to the protein concentration.

Statistical Analysis

All data and results were confirmed in at least 3 independent experiments. Statistical significance was determined by one-way analysis of variance (ANOVA).

Results

KPNA2 Overexpression in Proliferative Disorders of the Skin

To investigate KPNA2 expression in various epidermal-proliferative disorders of the skin, immunohistochemical staining of KPNA2 was performed on biopsy specimens of epidermal tumors as well as psoriasis and atopic dermatitis, which are inflammatory skin diseases with higher and lower epidermal proliferation, respectively. KPNA2 staining was faint and homogeneous without significant nuclear accumulation in healthy epidermis. In contrast, there was marked KPNA2 staining in the nuclei and cytoplasm of malignant cells in several skin tumors with different prognoses including Bowen's disease, actinic keratosis, squamous cell carcinoma (SCC), Paget's disease, Merkel cell carcinoma, and Mycosis fungoides. In malignant cells of SCC *in situ* such as Bowen's disease and actinic keratosis as with well prognosis, KPNA2 expressed predominantly in the basal layer. In contrast, established SCC showed rather intense and diffuse expression of KPNA2 in the malignant cells. Non-squamous cell malignant tumors of the skin including Paget's disease, Merkel cell carcinoma, and mycosis fungoides also showed diffuse, intense staining of KPNA2, indicating significantly higher expression in skin malignancy. Marked staining of KPNA2 was also observed in psoriatic skin, but was limited to the cytoplasm of basal layer keratinocytes. In contrast, very few but significant numbers of KPNA2-positive keratinocytes were observed in the basal lesions of atopic dermatitis, particularly in the inflamed proliferating lesions (**Figure 1**).

Contribution of KPNA2 and other KPNAs to Keratinocyte Cell Growth

To assess the role of KPNs in keratinocyte proliferation, HaCaT cell growth in culture was assessed by MTS assay after siRNA-mediated knockdown of KPNs. In culture medium containing 10% FBS, growth was significantly suppressed by KPNB1 knockdown [13]; however, knockdown of other KPNAs produced no significant effect (data not shown). In starved culture medium with 0.1% FBS, HaCaT cell growth was significantly suppressed by siRNA knockdown of KPNA1, 2, 3, and 4, suggesting adequate expression of KPNAs may be required for growth maintenance, especially in starved cells such as cancer cells. About 20% of HaCaT keratinocyte growth was suppressed 120 h after KPNA knockdown. KPNA siRNAs were individually subtracted from the siRNA cocktail to investigate the contribution of each KPNA to growth suppression. Interestingly, only KPNA2 siRNA subtraction resulted in the significant recovery of cell growth up to the control level (**Figure 2**), while removal of the other KPNA siRNAs did not affect growth suppression (data not shown). KPNA2 knockdown alone had no significant growth suppression effect, suggesting the other KPNAs are redundant. These data suggest KPNAs complement each other during cell growth, but KPNA2 may be essential for maintaining cell proliferation under starvation conditions.

Association of KPNA2 with Ribosomal Proteins in the Nucleolus

To identify proteins that interact with KPNA2 in HaCaT keratinocytes, we used the TAP method, which enabled us to easily isolate and purify proteins bound to the stably expressed TAP-tagged target recombinant protein [22,23]. Proteins associated with the KPNA2-TAP complex were isolated from the nuclei and cytoplasm of KPNA2-TAP-expressing HaCaT cells, separated

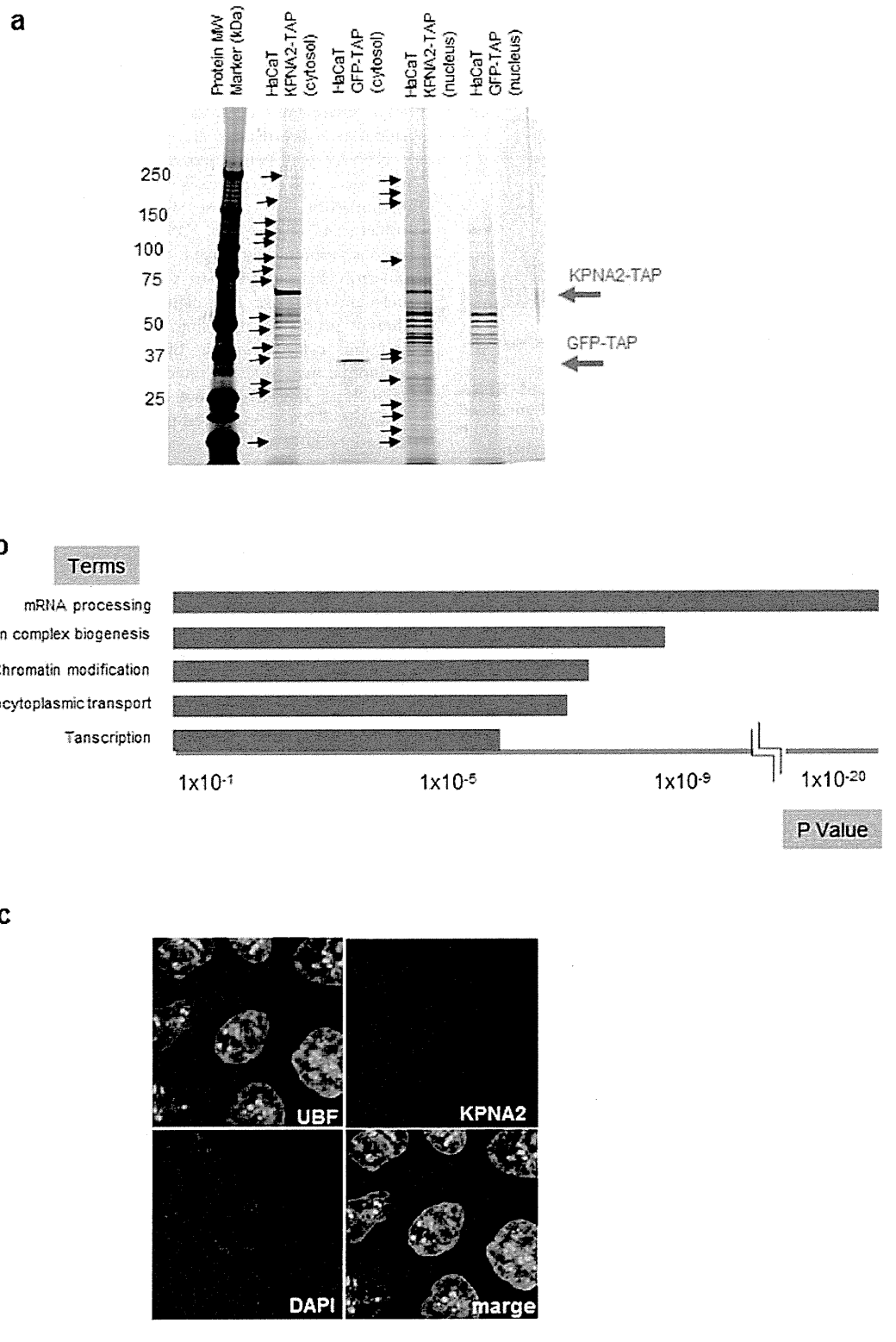

Figure 3. Detection and analysis of proteins that interact with KPNA2 and localization of KPNA2 in the nucleolus. Proteins that interact with KPNA2 in the cytoplasm and nucleus were purified using the TAP method and detected by silver staining. Proteins marked with arrows were analyzed by LC/MS/MS. HaCaT cells expressing GFP-TAP were used to detect nonspecific interactions. **a)** The results of LC/MS/MS were analyzed by pathway analysis using reactome (http://www.reactome.org). The categories of "mRNA processing", "ribonucleoprotein complex biogenesis", "chromatin modification," and "transcription" were the most significantly represented pathways. **b)** Immunohistochemistry revealed KPNA2 co-localization with UBF, a nucleolar marker.
doi:10.1371/journal.pone.0076416.g003

Table 1. Lists of proteins analyzed by pathway analysis.

mRNA processing	
RALY	RNA-binding protein Raly
NCBP1	Nuclear cap-binding protein subunit 1
RNMT	mRNA cap guanine-N7 methyltransferase
GAR1	H/ACA ribonucleoprotein complex subunit 1
PABPC4	PABPC4 protein
MLH1	DNA mismatch repair protein Mlh1
YBX1	Nuclease-sensitive element-binding protein 1
SRRT	Serrate RNA effector molecule homolog
DDX17	Probable ATP-dependent RNA helicase DDX17
RRP1B	Ribosomal RNA processing protein 1 homolog B
PCBP1	Poly(rC)-binding protein 1
PCBP2	Poly(rC)-binding protein 2
SFRS9	Splicing factor, arginine/serine-rich 9
PABPC1	Polyadenylate-binding protein 1
NSUN2	tRNA (cytosine-5-)-methyltransferase NSUN2
KRR1	KRR1 small subunit processome component homolog
DHX9	ATP-dependent RNA helicase A
RRP1	Ribosomal RNA processing protein 1 homolog B
DDX1	ATP-dependent RNA helicase DDX1
HNRNPU	Heterogeneous nuclear ribonucleoprotein U
TTF2	Transcription termination factor 2
SFRS3	Splicing factor, arginine/serine-rich 3
PHAX	Phosphorylated adapter RNA export protein
NOP2	Putative ribosomal RNA methyltransferase NOP2
RPS16	RPS16 protein
SNRNP200	U5 small nuclear ribonucleoprotein 200 kDa helicase
SYF2	Pre-mRNA-splicing factor SYF2
NOP56	NOP56 protein
RBM14	RNA-binding protein 14
BAT1	Spliceosome RNA helicase BAT1
ADAR	Double-stranded RNA-specific adenosine deaminase
KIAA1429	Protein virilizer homolog
Ribonucleoprotein complex biogenesis	
NCBP1	Nuclear cap-binding protein subunit 1
KRR1	KRR1 small subunit processome component homolog
RRP1	Ribosomal RNA processing protein 1 homolog B
GAR1	H/ACA ribonucleoprotein complex subunit 1
NIP7	60 S ribosome subunit biogenesis protein NIP7 homolog
DDX1	ATP-dependent RNA helicase DDX1
PHAX	Phosphorylated adapter RNA export protein
NOP2	Putative ribosomal RNA methyltransferase NOP2
RPS16	RPS16 protein
RRP1B	Ribosomal RNA processing protein 1 homolog B
SNRNP200	U5 small nuclear ribonucleoprotein 200 kDa helicase
SFRS9	Splicing factor, arginine/serine-rich 9
NOP56	NOP56 protein
Chromatin modification	

Table 1. Cont.

mRNA processing	
ING5	Inhibitor of growth protein 5
RBBP4	Histone-binding protein RBBP4
RBBP7	Histone-binding protein RBBP7
ARID2	AT-rich interactive domain-containing protein 2
CHD8	Chromodomain-helicase-DNA-binding protein 8
HDAC2	Histone deacetylase 2
HDAC1	Histone deacetylase 1
ASH1L	Probable histone-lysine N-methyltransferase ASH1L
BRDT	Bromodomain testis-specific protein
RBM14	RNA-binding protein 14
BCOR	BCL-6 corepressor
CHD4	Chromodomain-helicase-DNA-binding protein 4
MLL2	Histone-lysine N-methyltransferase MLL2
Nucleocytoplasmic transport	
PHAX	Phosphorylated adapter RNA export protein
NCBP1	Nuclear cap-binding protein subunit 1
UPF1	Regulator of nonsense transcripts 1
SET	Protein SET
GLE1	Nucleoporin GLE1
NUPL2	Nucleoporin-like protein 2
TPR	Nucleoprotein
KPNA2	Importin subunit alpha-2
KPNB1	Importin subunit beta-1
BAT1	Spliceosome RNA helicase BAT1
Transcription	
ING5	Inhibitor of growth protein 5
NMI	N-myc-interactor
FOXK1	Forkhead box protein K1
FOXM1	Forkhead box protein M1
CCNT1	Cyclin-T1
ARID2	AT-rich interactive domain-containing protein 2
YBX1	Nuclease-sensitive element-binding protein 1
CNOT4	CCR4-NOT transcription complex subunit 4
YBX2	Y-box-binding protein 2
CHD8	Chromodomain-helicase-DNA-binding protein 8
ASH2L	Set1/Ash2 histone methyltransferase complex subunit ASH2
BCOR	BCL-6 corepressor
EWSR1	RNA-binding protein EWS
CHD4	Chromodomain-helicase-DNA-binding protein 4
MLL2	Histone-lysine N-methyltransferase MLL2
ASXL3	Putative Polycomb group protein ASXL3
TAF4	Transcription initiation factor TFIID subunit 4
RBBP4	Histone-binding protein RBBP4
TAF6	Transcription initiation factor TFIID subunit 6
POLR1A	DNA-directed RNA polymerase I subunit RPA1
MED12	Mediator of RNA polymerase II transcription subunit 12
CSDA	DNA-binding protein A

doi:10.1371/journal.pone.0076416.t001

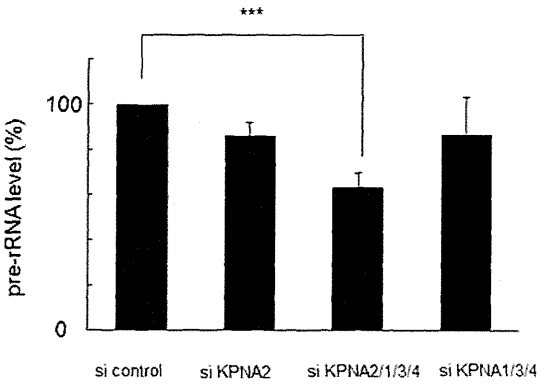

Figure 4. Suppression of ribosomal RNA synthesis by combined KPNA knockdown. Under starvation conditions (0.1% fetal bovine serum), siRNA-mediated knockdown of KPNA2, 1, 3, and 4 significantly suppressed ribosomal RNA synthesis analyzed by reverse transcription-quantitative polymerase chain reaction (***p<0.01). The amount of pre-ribosomal RNA was reduced by about 37% after 72 h.
doi:10.1371/journal.pone.0076416.g004

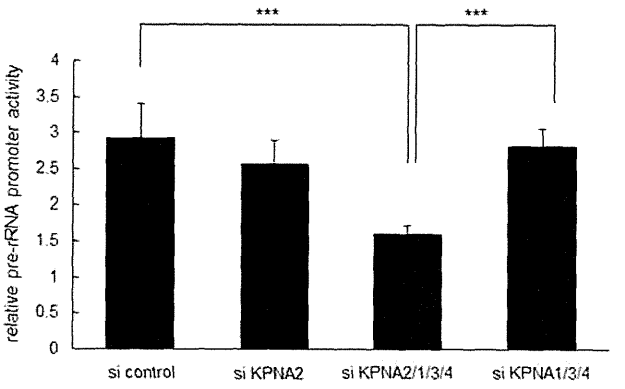

Figure 6. Suppression of the pre-ribosomal RNA promoter by combined KPNA knockdown. Under starvation conditions (0.1% fetal bovine serum), siRNA-mediated knockdown of KPNA2, 1, 3, and 4 significantly suppressed pre-rRNA promoter activity after 24 h (***p<0.01).
doi:10.1371/journal.pone.0076416.g006

by SDS-PAGE, and silver stained. HaCaT cells expressing GFP-TAP were used as a negative control (**Figure 3a**). KPNA2-TAP-associated proteins extracted from the silver-stained gel were identified by mass spectrometry. Numerous proteins were analyzed by reactome (http://www.reactome.org) to investigate their biological relationships. Pathway analysis revealed that the proteins interacting with KPNA2 were associated with mRNA processing, ribonucleoprotein complex biogenesis, chromatin modification, and transcription, all of which are essential for cell activities including cell growth (**Figure 3b, Table 1**). Interestingly, significant numbers of ribosomal proteins were listed as associated with KPNA2. Furthermore, immunofluorescence staining of KPNA2 in cultured HaCaT keratinocytes demonstrated co-localization of KPNA2 with UBF in the nucleoli, suggesting a role of KPNA2 for maintaining rRNA function (**Figure 3c**).

Contribution of KPNA2 to Protein Synthesis and Ribosomal RNA Transcription

Because the nucleolus is specifically responsible for rRNA transcription and maintenance of gene expression/transcription and mRNA processing, we hypothesized that KPNA2 in the nucleoli may regulate rRNA transcription to maintain cell growth under starvation conditions. To test this hypothesis, the siRNA cocktail was again applied to knockdown KPNAs to observe the effect on pre-rRNA transcription in starved HaCaT keratinocytes. Knockdown of all KPNAs reduced pre-rRNA levels as measured by RT-qPCR. In the 72 h after treatment with the siRNA cocktail, pre-rRNA expression was reduced by about 40%. Subtraction of KPNA2 siRNA restored pre-rRNA expression. The other KPNAs did not contribute to pre-rRNA expression. Treatment with KPNA2 siRNA alone had no significant effect, suggesting a redundant mechanism with other KPNAs (**Figure 4**). Protein synthesis in HaCaT keratinocytes was also reduced, corresponding to the suppression of pre-rRNA expression (**Figure 5**). The pre-rRNA promoter was also suppressed by KPNA knockdown after 24 h (**Figure 6**). Fluorescence-activated cell sorting of HaCaT cells before and after KPNA knockdown showed no significant change in the cell cycle pattern (data not shown). These data suggest KPNA2 might positively regulate rRNA transcription in the nucleolus, maintaining cell growth by ensuring transcription and translation directly or indirectly.

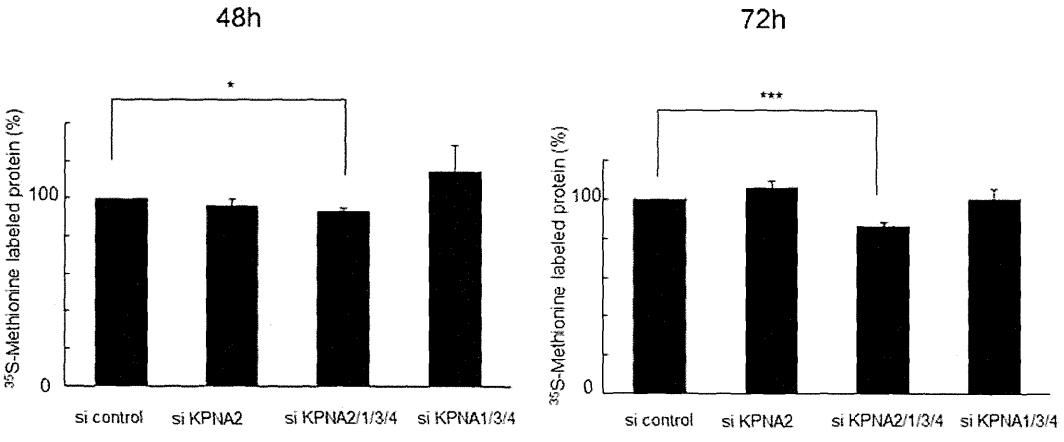

Figure 5. Suppression of protein synthesis by combined KPNA knockdown. Under starvation conditions (0.1% fetal bovine serum), siRNA-mediated knockdown of KPNA2, 1, 3, and 4 significantly suppressed protein synthesis after 48 h (*p<0.05) and 72 h (***p<0.01), as demonstrated by metabolic labeling with ^{35}S-methionine.
doi:10.1371/journal.pone.0076416.g005

Discussion

In this study, KPNA2 was overexpressed in proliferating disorders of the skin and interacted with many kinds of proteins that control transcription and gene expression directly and indirectly. This was the first report to show that KPNA2 is essential for cell growth in terms of rRNA and protein synthesis under starvation conditions.

KPNA2 overexpression in several skin malignancies is associated with varying prognoses. In the basal cells of psoriasis, KPNA2 expression was diffusely up-regulated in comparison to atopic dermatitis. Thus, KPNA2 expression might be induced in cells in which proliferation has been activated. Comparing Bowen's disease and actinic keratosis, which are known as SCC *in situ*, KPNA2 was remarkably and diffusely overexpressed. KPNA2 may therefore be a tumor marker with utility as a prognostic factor of proliferative activity in skin malignancies, although we have insufficient sample sizes to determine significance. Previous reports have demonstrated KPNA2 overexpression in various tumors cells *in vitro* and *in vivo*; elevated KPNA2 and KPNB1 expression in cancer cells correlates with altered transcriptional regulation associated with deregulated E2F/Rb activities [26]. Some studies have indicated that higher KPNA2 expression in tumor cell nuclei shortens patient survival, although the mechanisms and precise roles of KPNA2 in the tumor cells remained unclear [16,17]. Researchers also hypothesized that KPNA2-mediated nuclear transport of proteins necessary for maintaining cell proliferation, such as transcription factors, promote tumor cell growth. In this context, KPNA2 was shown to interact with NBS1 (Nijmegen breakage syndrome 1), a key regulator of the MRE11/RAD50/NBS1 complex. NBS1 promotes tumorigenesis by binding and activating the phosphatidylinositol 3-kinase/AKT pathway [27]. Interestingly, siRNA-medicated KPNA2 knockdown studies revealed a different cellular response to KPNA2 inhibition in prostate and cervical cancer cell lines. In prostate cell line PC3, proliferation and viability were significantly reduced when KPNA2 expression was inhibited, whereas there was no significant change in a cervical cancer cell line. This difference could be due to tissue-specific tumor etiologies [13,17].

In this study, we characterized KPNA2-binding proteins *in situ* in immortalized HaCaT keratinocytes. In silico gene ontology indicated a significant relationship between KPNA2 binding proteins and mRNA processing, ribonucleoprotein complex biogenesis, chromatin modification, and transcription. KPNA2 interacted with various ribosomal proteins and heterogeneous nuclear ribonucleoproteins directly or indirectly and was located in the nucleolus, the site of pre-rRNA transcription and processing and ribosome assembly. rRNA synthesis, the first event in ribosome synthesis, is a fundamental determinant of a cell's capacity to grow and proliferate. Ribosomal RNA genes (rDNAs) are transcribed with high efficiency and the complex regulation of rRNA synthesis is responsive to general metabolism and specific environmental challenges [20,28]. Serum starvation is also a well-established approach to inducing a broad range of cellular stress. TAP analysis revealed that KPNA2 associates with numerous ribosomal RNA synthesis-related proteins including RNA polymerase I subunit, rRNA methyl transferase, rRNA subunit biogenesis protein, and rRNA processing proteins. Furthermore, KPNA2 accumulates in the nucleolus and contributes to rRNA transcription *in vitro*. These lines of evidence suggest KPNA2 may serve important roles as a canonical nuclear transporter and to ensure rRNA biogenesis in proliferating cells. In this context, enhanced KPNA2 expression in malignant and inflammatory keratinocytes may positively regulate their proliferating capacity by supporting rRNA synthesis, which is indispensable. In malignant cells, the poor prognosis indicated by nuclear KPNA2 accumulation may be associated with KPNA2 retention in response to cellular stress and increasing rRNA synthesis or changing gene expression.

KPNA subtypes exhibit different abilities to interact with specific NLS-containing cargos and in various expression patterns in cells and tissues. KPNA2 is highly expressed in undifferentiated embryonic stem cells and down-regulated during neural differentiation, indicating that proper expression of KPNA2 is required for embryonic stem cells to maintain their undifferentiated state [29]. KPNs are also complementary because they are indispensable for cellular proliferation and differentiation. We previously examined the effect of KPNA2 siRNA subtraction on RNA expression in normal human keratinocytes by microarray analysis [4]; however, there was no increases of more than 2 fold in any other KPNs including KPNA1, 3, 4, and KPNB1 (data not shown).

In this study, KPNA2 was essential for cell growth related to rRNA and protein synthesis under starvation conditions; however, there was no significant change when only KPNA2 was knocked down. Combined knockdown of KPNA2, 1, 3, and 4 was needed to suppress cell growth and KPNA2 was indispensable. Even under these conditions, growth suppression was gradual and mild over 120 h. Furthermore, combined knockdown of KPNAs mildly suppressed the synthesis of rRNA and proteins after 72 h. These results indicated that KPNAs might play complementary roles with sufficient reserves.

Further studies are needed to clarify the additional function of KPNA2 in cell proliferation, which would be a focus for a new treatment to regulate KPNA2.

Acknowledgments

We sincerely appreciate the kind support of Prof. Yasufumi Kaneda. We also thank Ms. Eriko Nobuyoshi and Ms. Sayaka Matsumura for technical support with immunohistochemistry and reverse transcription-quantitative polymerase chain reaction.

Author Contributions

Conceived and designed the experiments: NU KT KN TN. Performed the experiments: NU SS. Analyzed the data: NU KT KN TN IK. Contributed reagents/materials/analysis tools: HN IK. Wrote the paper: NU KT.

References

1. Pemberton LF, Paschal BM (2005) Mechanisms of receptor-mediated nuclear import and nuclear export. Traffic 6: 187–198.
2. Yasuhara N, Oka M, Yoneda Y (2009) The role of the nuclear transport system in cell differentiation. Semin Cell Dev Biol 20: 590–599.
3. Yasuda Y, Miyamoto Y, Yamashiro T, Asally M, Masui A, et al. (2012) Nuclear retention of importin alpha coordinates cell fate through changes in gene expression. EMBO J 31: 83–94.
4. Umegaki N, Tamai K, Nakano H, Moritsugu R, Yamazaki T, et al. (2007) Differential regulation of karyopherin alpha 2 expression by TGF-beta1 and IFN-gamma in normal human epidermal keratinocytes: evident contribution of KPNA2 for nuclear translocation of IRF-1. J Invest Dermatol 127: 1456–1464.
5. Freire J, Covelo G, Sarandeses C, Diaz-Jullien C, Freire M (2001) Identification of nuclear-import and cell-cycle regulatory proteins that bind to prothymosin alpha. Biochem Cell Biol 79: 123–131.
6. Hall MN, Griffin CA, Simionescu A, Corbett AH, Pavlath GK (2011) Distinct roles for classical nuclear import receptors in the growth of multinucleated muscle cells. Dev Biol 357: 248–258.
7. Schatz CA, Santarella R, Hoenger A, Karsenti E, Mattaj IW, et al. (2003) Importin alpha-regulated nucleation of microtubules by TPX2. EMBO J 22: 2060–2070.

8. Gruss OJ, Carazo-Salas RE, Schatz CA, Guarguaglini G, Kast J, et al. (2001) Ran induces spindle assembly by reversing the inhibitory effect of importin alpha on TPX2 activity. Cell 104: 83–93.
9. Ems-McClung SC, Zheng Y, Walczak CE (2004) Importin alpha/beta and Ran-GTP regulate XCTK2 microtubule binding through a bipartite nuclear localization signal. Mol Biol Cell 15: 46–57.
10. Askjaer P, Galy V, Hannak E, Mattaj IW (2002) Ran GTPase cycle and importins alpha and beta are essential for spindle formation and nuclear envelope assembly in living Caenorhabditis elegans embryos. Mol Biol Cell 13: 4355–4370.
11. Harel A, Forbes DJ (2004) Importin beta: conducting a much larger cellular symphony. Mol Cell 16: 319–330.
12. Rotem A, Gruber R, Shorer H, Shaulov L, Klein E, et al. (2009) Importin beta regulates the seeding of chromatin with initiation sites for nuclear pore assembly. Mol Biol Cell 20: 4031–4042.
13. van der Watt PJ, Maske CP, Hendricks DT, Parker MI, Denny L, et al. (2009) The Karyopherin proteins, Crm1 and Karyopherin beta1, are overexpressed in cervical cancer and are critical for cancer cell survival and proliferation. Int J Cancer 124: 1829–1840.
14. Winnepenninckx V, Lazar V, Michiels S, Dessen P, Stas M, et al. (2006) Gene expression profiling of primary cutaneous melanoma and clinical outcome. J Natl Cancer Inst 98: 472–482.
15. Wang CI, Wang CL, Wang CW, Chen CD, Wu CC, et al. (2011) Importin subunit alpha-2 is identified as a potential biomarker for non-small cell lung cancer by integration of the cancer cell secretome and tissue transcriptome. Int J Cancer 128: 2364–2372.
16. Gluz O, Wild P, Meiler R, Diallo-Danebrock R, Ting E, et al. (2008) Nuclear karyopherin alpha2 expression predicts poor survival in patients with advanced breast cancer irrespective of treatment intensity. Int J Cancer 123: 1433–1438.
17. Mortezavi A, Hermanns T, Seifert HH, Baumgartner MK, Provenzano M, et al. (2011) KPNA2 expression is an independent adverse predictor of biochemical recurrence after radical prostatectomy. Clin Cancer Res 17: 1111–1121.
18. Noetzel E, Rose M, Bornemann J, Gajewski M, Knuchel R, et al. (2012) Nuclear transport receptor karyopherin-alpha2 promotes malignant breast cancer phenotypes in vitro. Oncogene 31: 2101–2114.
19. Tanaka Y, Okamoto K, Teye K, Umata T, Yamagiwa N, et al. (2010) JmjC enzyme KDM2A is a regulator of rRNA transcription in response to starvation. EMBO J 29: 1510–1522.
20. Grummt I (2003) Life on a planet of its own: regulation of RNA polymerase I transcription in the nucleolus. Genes Dev 17: 1691–1702.
21. Murayama A, Ohmori K, Fujimura A, Minami H, Yasuzawa-Tanaka K, et al. (2008) Epigenetic control of rDNA loci in response to intracellular energy status. Cell 133: 627–639.
22. Rigaut G, Shevchenko A, Rutz B, Wilm M, Mann M, et al. (1999) A generic protein purification method for protein complex characterization and proteome exploration. Nat Biotechnol 17: 1030–1032.
23. Nimura K, Ura K, Shiratori H, Ikawa M, Okabe M, et al. (2009) A histone H3 lysine 36 trimethyltransferase links Nkx2–5 to Wolf-Hirschhorn syndrome. Nature 460: 287–291.
24. Shevchenko A, Wilm M, Vorm O, Mann M (1996) Mass spectrometric sequencing of proteins silver-stained polyacrylamide gels. Anal Chem 68: 850–858.
25. Ghoshal K, Majumder S, Datta J, Motiwala T, Bai S, et al. (2004) Role of human ribosomal RNA (rRNA) promoter methylation and of methyl-CpG-binding protein MBD2 in the suppression of rRNA gene expression. J Biol Chem 279: 6783–6793.
26. van der Watt PJ, Ngarande E, Leaner VD (2011) Overexpression of Kpnbeta1 and Kpnalpha2 importin proteins in cancer derives from deregulated E2F activity. PLoS One 6: e27723.
27. Teng SC, Wu KJ, Tseng SF, Wong CW, Kao L (2006) Importin KPNA2, NBS1, DNA repair and tumorigenesis. J Mol Histol 37: 293–299.
28. Moss T (2004) At the crossroads of growth control; making ribosomal RNA. Curr Opin Genet Dev 14: 210–217.
29. Yasuhara N, Shibazaki N, Tanaka S, Nagai M, Kamikawa Y, et al. (2007) Triggering neural differentiation of ES cells by subtype switching of importin-alpha. Nat Cell Biol 9: 72–79.

IJC
International Journal of Cancer

New findings of kinase switching in gastrointestinal stromal tumor under imatinib using phosphoproteomic analysis

Tsuyoshi Takahashi[1,2], Satoshi Serada[2], Maiko Ako[2], Minoru Fujimoto[2], Yasuaki Miyazaki[1], Rie Nakatsuka[1,2], Takayuki Ikezoe[3], Akihito Yokoyama[3], Takahiro Taguchi[4], Kazuki Shimada[5], Yukinori Kurokawa[1], Makoto Yamasaki[1], Hiroshi Miyata[1], Kiyokazu Nakajima[1], Shuji Takiguchi[1], Masaki Mori[1], Yuichiro Doki[1], Tetsuji Naka[2] and Toshirou Nishida[2,6]

[1] Department of Surgery, Osaka University Graduate School of Medicine, Suita, Japan
[2] Laboratory for Immune Signal, National Institute of Biomedical Innovation, Ibaraki, Japan
[3] Department of Hematology and Respiratory Medicine, Kochi Medical School, Kochi University, Nankoku, Japan
[4] Research and Education Faculty, Multidisciplinary Science Cluster, Kuroshio Science Unit, Kochi Medical School, Kochi University, Nankoku, Japan
[5] Department of Respiratory Medicine, Allergy and Rheumatic Diseases, Osaka University Graduate School of Medicine, Suita, Japan
[6] Department of Surgery, Osaka Police Hospital, Osaka, Japan

Despite the revolutionary effects of imatinib on advanced gastrointestinal stromal tumors (GISTs), most patients eventually develop disease progression following primary resistance or acquired resistance driven by secondary-resistant mutations. Even in radiographically vanishing lesions, pathology has revealed persistent viable cells during imatinib therapy, which could lead to the emergence of drug-resistant clones. To uncover the mechanisms underlying these clinical issues, here we examined imatinib-induced phosphoproteomic alterations in GIST-T1 cells, using our quantitative tyrosine phosphoproteomic analysis method, which combined immunoaffinity enrichment of phosphotyrosine-containing peptides with isobaric tags for relative and absolute quantitation (iTRAQ) technology. Using this approach, we identified 171 tyrosine phosphorylation sites spanning 134 proteins, with 11 proteins exhibiting greater than 1.5-fold increases in tyrosine phosphorylation. Among them, we evaluated FYN and focal adhesion kinase (FAK), both of which are reportedly involved in proliferation and malignant alteration of tumors. We confirmed increased tyrosine phosphorylation of both kinases by western blotting. Inhibition of FYN and FAK phosphorylation each increased tumor cell sensitivity to imatinib. Furthermore, a FAK-selective inhibitor (TAG372) induced apoptosis of imatinib-resistant GIST-T1 cells and decreased the imatinib IC_{50}. These results indicate that FYN or FAK might be potential therapeutic targets to overcome resistance to imatinib in GISTs. Additionally, we showed that the iTRAQ-based quantitative phosphotyrosine-focused phosphoproteomic approach is a powerful method for screening phosphoproteins associated with drug resistance.

The gastrointestinal stromal tumor (GIST) is the most common mesenchymal tumor of the digestive tract, and is characterized by expression of the KIT (CD117) and/or DOG1 proteins. Most GISTs have oncogenic *KIT* or *PDFGRA* mutations, which is a key factor in sporadic GIST pathogenesis and proliferation.[1–3] This knowledge has facilitated the development of targeted therapies with tyrosine kinase inhibitors and led to the revolutionary treatment with imatinib mesylate (Glivec®; Novartis Pharmaceuticals). Recent clinical trials with advanced/unresectable GIST have shown that imatinib produces objective responses in ~50% of patients, and disease stabilization (stable disease) in another 30–40%. The corresponding 2-year overall survival rates range from 70 to 80%, indicating markedly improved patient outcomes compared with anecdotal data from cytotoxic chemotherapy in the preimatinib era.[4–6]

Despite imatinib's effectiveness, there remain several problems. First, GIST patients cannot stop taking the drug even if complete response is obtained, because discontinuation inevitably leads to reprogression and disease relapse.[7,8] Second, imatinib activity is limited by primary resistance to the drug in ~15% of patients, and secondary resistance eventually develops in more than 80% of patients.[5,9] Secondary resistance mainly occurs due to additional kinase domain mutations, which are thought to develop in viable tumor cells (persistent cells) during imatinib therapy. It is not yet known

Key words: GIST, imatinib, iTRAQ, proteomics

Abbreviations: FAK: focal adhesion kinase; GIST: gastrointestinal stromal tumor; iTRAQ: isobaric tags for relative and absolute quantitation; LC: liquid chromatography; MS/MS: tandem mass spectrometry; shRNA: small hairpin RNA; siRNA: small interfering RNA

Additional Supporting Information may be found in the online version of this article.

DOI: 10.1002/ijc.28282
History: Received 17 Dec 2012; Accepted 2 May 2013; Online 28 May 2013

Correspondence to: Toshirou Nishida, Department of Surgery, Osaka Police Hospital, 10-31, Kitayama-cho, Tennoji-ku, Osaka 543-0035, Japan, Tel.: +81-6-6771-6051, Fax: +81-6-6775-2838, E-mail: toshin@mvb.biglobe.ne.jp

What's new?
While the targeted tyrosine kinase inhibitor imatinib can significantly improve two-year survival rates for patients with gastrointestinal stromal tumor (GIST), primary and secondary resistance mutations often limit its benefits. This study of the human GIST-T1 cell line suggests that imatinib-induced increases in tyrosine phosphorylation of FYN kinase and focal adhesion kinase (FAK) may be responsible for mediating some instances of imatinib resistance and therefore may be potential targets for killing persistent tumor cells and overcoming resistance. The findings also indicate that iTRAQ-based quantitative phosphotyrosine-focused proteomic analysis is a useful way of screening for phosphoproteins associated with drug resistance.

what mechanisms keep these persistent cells alive after shutdown of KIT signaling by imatinib.

Phosphorylation of protein kinases in signaling pathways is a key event in tumor cell survival and proliferation. Differential phosphoprotein analysis may provide clues to alternatively activated pathways and/or substituted kinases that may be activated after inhibition of main pathways, such as KIT.[10] Recent advances in mass spectrometry-based phosphoproteomics enable extensive profiling of serine-threonine kinases, while tyrosine kinase analysis has remained challenging in terms of quantity and quality. However, a recent method coupling peptide-level antiphosphotyrosine immunoaffinity purification with liquid chromatography (LC)-tandem mass spectrometry (MS/MS) has provided reasonable profiling for tyrosine phosphorylation.[11]

In the present study, we quantitatively measured the phosphoproteomic alterations induced by imatinib in a GIST-T1 cell line. We also examined the roles of some tyrosine kinases that were activated in persistent tumor cells after imatinib exposure.

Material and Methods

Cell lines

We previously established the human GIST cell line GIST-T1, which has a 57-nucleotide (V570-Y578) in-frame deletion in KIT exon 11.[12] The cell line identity was confirmed by DNA fingerprinting through short tandem repeat profiling, as previously described.[13] GIST-T1-R was established from GIST-T1 as an imatinib-resistant clone that arose from continuous culturing in 5 μM imatinib. The GIST-T1-R cells GIST-T1-R2 and GIST-T1-R8 each exhibit imatinib IC_{50} values of ~30 μM, which is ~1000 times that of the GIST-T1 parent.

Reagents and antibodies

Imatinib and TAG372—selective tyrosine kinase inhibitors for KIT and focal adhesion kinase (FAK), respectively—were synthesized and provided by Novartis Pharmaceuticals (Basel, Switzerland). The following primary antibodies were used: anti-phospho-Src Family (Tyr416) (1:1000), anti-phospho-ERK and anti-ERK from Cell Signaling Technology (Danvers, MA); anti-GAPDH from Santa Cruz Biotechnology (Santa Cruz, CA); anti-phospho-FAK (Tyr397) from Biosource (Camarillo, CA); anti-FAK from BD Transduction Laboratories (San Jose, CA) and anti-phosphotyrosine (clone 4G10) from Upstate Biotechnology (Lake Placid, NY). Detailed immunoprecipitation information is provided in the Supporting Information Materials and Methods section.

Peptide synthesis

A tyrosine-phosphorylated peptide (NVPLyK) derived from a trypsinized peptide sequence of yeast alpha-enolase was synthesized at Sigma Aldrich (Milwaukee, WI) using standard solid-phase peptide synthesis techniques and Fmoc chemistry.

Phosphopeptide immunoprecipitation

GIST-T1 cells were treated with 400 nM of imatinib for 0, 1, 6 and 24 hr. Tyrosine-phosphorylated peptides were purified using Cell Signaling PhosphoScan pTyr100 Kits (Beverly, MA) following the manufacturer's instructions with minor modification. Detailed information is provided in the Supporting Information Materials and Methods section.

iTRAQ labeling

After immunoprecipitation, peptides were dissolved in 9.8 M Urea (5 μL) and 1 M TEAB (20 μL). Following the manufacturer's protocol (Applied Biosystems, Foster City, CA), the samples were labeled with the isobaric tags for relative and absolute quantitation (iTRAQ) reagents as follows: GIST-T1 with reagent 114 (0 hr), GIST-T1 with reagent 115 (1 hr), GIST-T1 with reagent 116 (6 hr) and GIST-T1 with reagent 117 (24 hr). The labeled peptide samples were then pooled and desalted with Sep-Pak Light C18 Cartridges, and the peptides were dried in a SpeedVac. The labeled peptide mixtures were purified and fractionated into 14 fractions using strong cation exchange fractionation, as previously described.[13]

Quantitative mass spectrometric analysis

Nano LC-MS/MS analysis and iTRAQ data analysis were performed as described in the Supporting Information Materials and Methods section.

Small interfering RNA transfection

Commercial FAK small interfering RNA (siRNA) and nonspecific siRNA were obtained from QIAGEN. Cells were transfected with siRNA using Lipofectamine 2000 reagent

(Invitrogen) following the manufacturer's instructions. Selective silencing of FAK was confirmed by western blot analysis.

Generation of FYN knockdown cells

To generate stable FYN knockdown cell lines, GIST-T1 cells were transfected with a commercial plasmid containing an anti-FYN short hairpin RNA (shRNA Fyn, plasmid KH00147N; SABiosciences [Qiagen], Frederick, MD) using Lipofectamine 2000 (Invitrogen, Carlsbad, CA) according to the manufacturer's instructions. The correctly transfected and expressing cells were selected with 600 μg/mL G418 (Invitrogen). Stable clones were maintained in 250 μg/mL G418. Three stable GIST-T1-FYN shRNA cell lines were established, designated B1, B2 and B3 cells. We also established a control cell line of GIST-T1 stably transfected with the empty vector, which we designated GIST-T1-C.

Measurement of IC_{50} after imatinib treatment

Cells were seeded in 96-well plates at 2000 cells/well (Costar; Corning, Corning, NY) for 24 hr and then exposed to various concentrations (0–40 μM) of imatinib for 72 hr. Cell proliferation was evaluated with the WST-8 [2-(2-methoxy-4-nitrophenyl)-3-(4-nitrophenyl)-5-(2,4-disulfophenyl)-2H-tetrazolium, monosodium salt] assay (Cell Counting Kit-SF; Nacalai Tesque) at the indicated post-treatment times. A microplate reader Model 680 (Bio-Rad Laboratories, Hercules, CA) was used to measure WST-8 absorption at a wavelength of 450 nm with a reference wavelength of 630 nm. Growth rate was expressed as the percentage of absorbance for treated cells vs. control cells. Experiments were performed in triplicate in two independent experiments, and the presented values are the averages of all six wells.

Apoptosis assay

GIST-T1 cells were seeded in 6-well plates at a density of 3×10^5 cells per well and treated with imatinib and/or TAG372 for 2 days. The cells were then washed with PBS, and caspase-3 activity was detected using the caspase-3 fluorometric assay kit (R&D systems, Minneapolis, MN) following the manufacturer's instructions. The presented values are the means of three independent experiments.

Statistical analysis

Statistical analyses were performed using the Mann–Whitney *U*-test or one-way analysis of variance (ANOVA), followed by Scheffe's test. One-way ANOVA followed by Dunnett's test was used for multiple comparisons.

Results

Quantitative phosphotyrosine proteomic analysis identifies upregulation of FYN and FAK in imatinib-exposed GIST-T1 cells

GIST-T1 cells that possessed the activating mutation in exon 11 of *KIT* are sensitive to imatinib, with a K_i value for imatinib of 20 nM. Time-dependent decreases in the tyrosine phosphorylation of KIT were observed when GIST-T1 cells were treated with 400 nM imatinib for 0, 1, 6 and 24 hr (Fig. 1*a*). These time-points were used for subsequent MS analysis, with 0 hr used as a control.

By utilizing immunoaffinity enrichment of phosphotyrosine peptides with quantitative phosphoproteomic analysis using iTRAQ technology combined with nano LC-MS/MS analysis, we identified 171 tyrosine phosphorylation sites spanning 134 proteins (Supporting Information Table S1). After imatinib treatment, a total of 11 phosphotyrosine sites spanning 11 proteins exhibited increases of >1.5-fold and 21 phosphotyrosine sites spanning 15 proteins showed decreases of <0.3-fold (Table 1). As a representative protein, we confirmed a dramatic decrease in the tyrosine phosphorylation levels of the KIT protein (Y609, Y703, Y747, Y823 and Y936). In contrast, imatinib induced increased phosphorylation of FYN (Y420) and FAK (Y576). Phosphorylation of FYN (Y420) upregulates tyrosine kinase activities, and phosphorylation of FAK (Y576) is critical for its maximal catalytic activity.

To validate these results obtained from iTRAQ analysis, we further examined the tyrosine phosphorylation of FYN and FAK using western blotting. As shown in iTRAQ analysis, western blotting confirmed that FYN (Y420) and FAK (Y576) were time dependently phosphorylated (Figs. 1*b* and 2*c*). When tyrosine phosphorylation in the activation loop was measured for other Src family kinases, we found that imatinib treatment did not increase tyrosine phosphorylation of SRC, LYN, LCK or YES (Fig. 1*b*).

Inhibition of FYN or FAK enhances imatinib sensitivity of GIST-T1 cells

To examine the functions of FYN in GIST-T1 cells exposed to imatinib, FYN expression was stably suppressed using a FYN shRNA plasmid. We cloned and established GIST-T1 B1, B2 and B3 cells, as well as GIST-T1 C cells transfected with empty vector as a control (Fig. 1*d*). Compared with GIST-T1 C cells, the FYN knockdown cell lines showed significantly decreased IC_{50} values for imatinib ($p < 0.05$; Fig. 1*d*).

We also examined the role of FAK activation in imatinib treatment. We repressed FAK expression using siRNA, and we used a FAK inhibitor (TAG372) to inhibit FAK phosphorylation. Transfection of FAK siRNA reduced IC_{50} values for imatinib ($p < 0.05$; Fig. 1*e*). When used with imatinib, TAG372 further decreased cell survival in a dose-dependent manner (Fig. 1*f*).

Inhibition of FAK improves imatinib sensitivity in GIST-T1-R cells

Next, we examined FAK activation in imatinib-resistant cell lines established from GIST-T1 cells. Eight imatinib-resistant cell lines were established by incubation of GIST-T1 cells with imatinib of gradually increased concentrations. Constitutive phosphorylation of FAK was observed in two imatinib-resistant

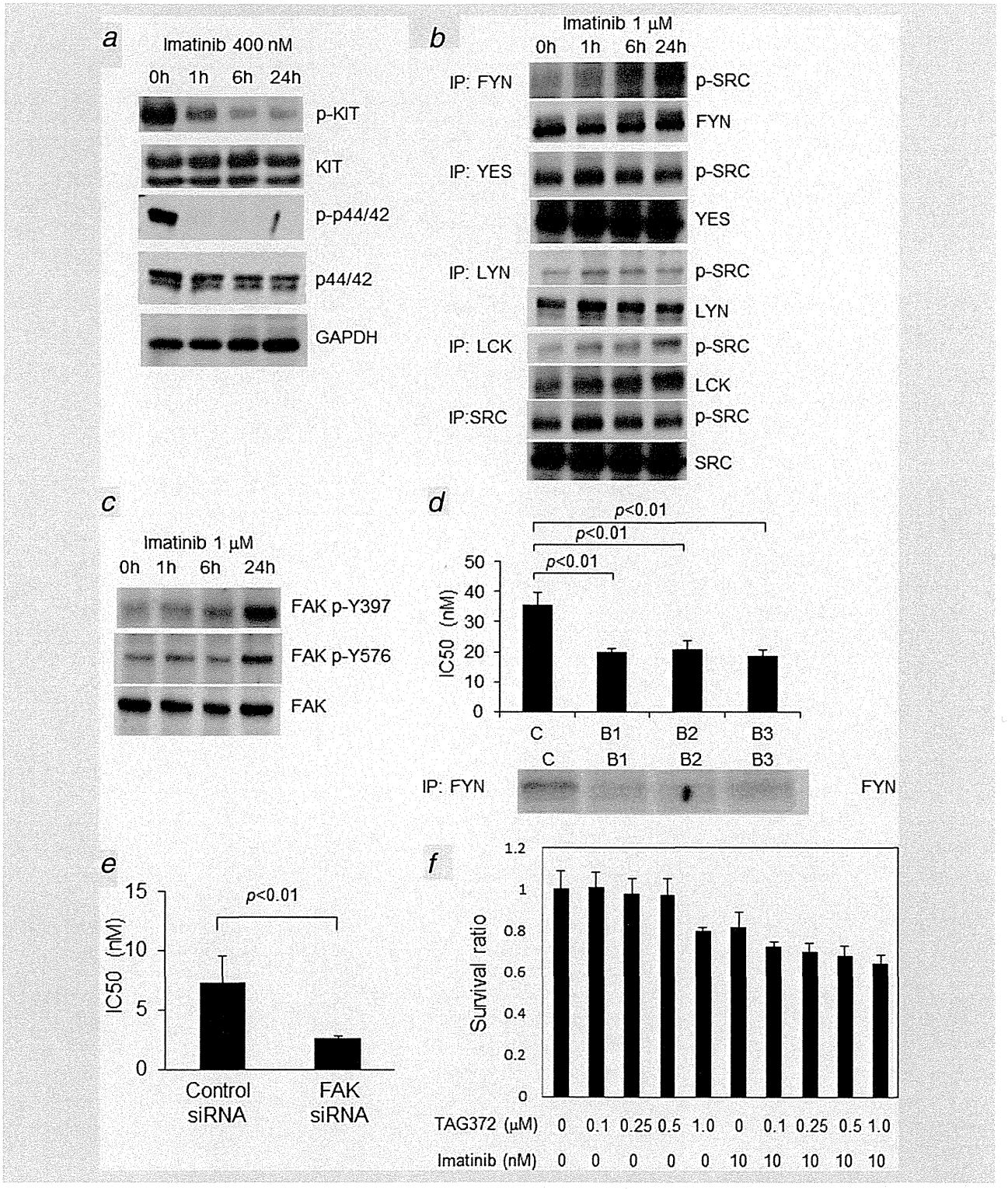

Figure 1. (*a*) Altered tyrosine phosphorylation levels detected by iTRAQ analysis were confirmed by western blotting. Imatinib treatment led to reduced phosphotyrosine levels. (*b*) Imatinib treatment changed SRC family kinase phosphorylation levels. (*c*) iTRAQ analysis showed that FYN (Y420) and FAK (Y576) exhibited similar tyrosine phosphorylation. (*d*) Compared with in GIST-T1 C cells, the IC_{50} for imatinib was significantly reduced in all FYN knockdown GIST-T1 cells (B1, B2 and B3). (*e*) The IC_{50} for imatinib was reduced in GIST-T1 cells that were transfected with FAK siRNA. (*f*) WST-8 assay showed the cell viability with imatinib and TAG372 treatment. Data are presented as means ± SD.

Table 1. Phosphotyrosine peptides that were increased or decreased by imatinib treatment, as quantified by iTRAQ analysis[1]

Accession Number	Sequence	Description	Site	1 hr/0 hr[2]	6 hr/0 hr[2]	24 hr/0 hr[2]
Greater than 1.5-fold increase of phosphorylated peptide at 24 hr compared with 0 hr						
P06241	LIEDNEYTAR	Tyrosine-protein kinase Fyn	Y420	0.845	2.365	3.641
P15880	AFVAIGDYNGHVGLGVK	40S ribosomal protein S2	Y133	2.138	1.807	2.443
O00401	VIYDFIEK	Neural Wiskott-Aldrich syndrome protein	Y256	0.768	1.491	1.978
Q99623	MLGEALSKNPGYIK	Prohibitin-2	Y248	1.446	1.778	1.726
P62829	NLYIISVK	60S ribosomal protein L23	Y38	2.138	1.348	1.679
P18433	VVQEYIDAFSDYANFK	Receptor-type tyrosine-protein phosphatase alpha	Y791	1.245	1.098	1.667
P30040	FDTQYPYGEK	Endoplasmic reticulum resident protein 29	Y64	1.804	2.558	1.640
Q05397	YMEDSTYYK	Focal adhesion kinase 1	Y570	1.043	0.893	1.606
A6NI28	LDTASSNGYQRPGSVVAAK	Rho GTPase-activating protein 42	Y792	0.599	0.980	1.594
P08758	LYDAYELK	Annexin A5	Y94	1.043	1.399	1.581
P18669	HYGGLTGLNK	Phosphoglycerate mutase 1	Y92	0.930	2.583	1.532
Less than 0.3-fold reduction of phosphorylated peptide at 24 hr compared with 0 hr						
P10721	IGSYIER	Mast/stem cell growth factor receptor Kit	Y747	0.649	0.244	0.291
O95490	SENEDIYYK	Latrophilin-2	Y1350	0.431	0.318	0.256
Q92569	LQEYHSQYQEK	Phosphatidylinositol 3-kinase regulatory subunit gamma	Y184	0.433	0.271	0.255
P10721	QEDHAEAALYK	Mast/stem cell growth factor receptor Kit	Y703	0.560	0.207	0.254
P10721	QISESTNHIYSNLANCSPNR	Mast/stem cell growth factor receptor Kit	Y936	0.445	0.212	0.244
Q92796	RDNEVDGQDYHFVVSR	Disks large homolog 3	Y673	0.556	0.427	0.241
Q5XXA6	STIVYEILKR	Anoctamin-1	Y251	0.508	0.720	0.235
Q00535	IGEGTYGTVFK	Cyclin-dependent kinase 5	Y15	1.877	0.821	0.232
Q06481	MQNHGYENPTYK	Amyloid-like protein 2	Y755	0.474	–[4]	0.220
O95297	INKSESVVYADIR	Myelin protein zero-like protein 1	Y263	0.785	0.249	0.211
Q969M3	QYAGYDYSQQGR	Protein YIPF5	Y42	0.145	–[4]	0.195
O14964	VVQDTYQIMK	Hepatocyte growth factor-regulated tyrosine kinase substrate	Y132	1.097	0.464	0.173
O95297	SESVVYADIR	Myelin protein zero-like protein 1	Y263	0.563	0.169	0.166
Q92569	VQAEDLLYGKPDGAFLIR	Phosphatidylinositol 3-kinase regulatory subunit gamma	Y373	1.186	0.176	0.130
O96000	YQDLGAYSSAR	NADH dehydrogenase [ubiquinone] 1 beta subcomplex subunit 10	Y143	0.864	0.393	0.122
P16333	LYDLNMPAYVK	Cytoplasmic protein NCK1	Y112	0.651	0.257	0.103
Q12846	NILSSADYVER	Syntaxin-4	Y251	0.179	0.131	0.072
Q8N128	YQYAIDEYYR	Protein FAM177A1	Y162	0.196	0.090	0.055
P10721	VVEATAYGLIK	Mast/stem cell growth factor receptor Kit	Y609	0.723	–[4]	0.023
P10721	DIKNDSNYVVK	Mast/stem cell growth factor receptor Kit	Y823	0.164	–[4]	–[4]
P53778	QADSEMTGYVVTR	Mitogen-activated protein kinase 12	Y185	1.582	0.888	–[4]

[1]The full list is provided in Supporting Information Table 1.
[2]The ratio of peptide derived from the iTRAQ reporter ion, as determined by iTRAQ analysis; 1 hr/0 hr, 6 hr/0 hr and 24 hr/0 hr refer, respectively, to the value of each peptide at 1, 6 and 24 hr divided by the value of that peptide at 0 hr.
[3]A 0-hr value of 0 (*i.e.* below background) and a positive value at 1, 6 or 24 hr.
[4]A 0-hr positive value and a value of 0 (*i.e.* below background) at 1, 6 or 24 hr.

GIST-T1 cell lines (GIST-T1-R2 and GIST-T1-R8), which had imatinib IC_{50} values of 30 μM, ~1000 times that of the GIST-T1 parent cells (Fig. 2*a*). TAG372 dose dependently inhibited FAK phosphorylation in GIST-T1-R2 (Fig. 2*b*), and significantly reduced the imatinib IC_{50} values when both drugs were used (Fig. 2*c*). Moreover, TAG372 induced apoptosis in GIST-T1-R2 (Fig. 2*d*). These results indicate that imatinib treatment induced activation of FYN and FAK in persistent GIST-T1 cells and was associated with imatinib insensitivity and resistance.

Discussion

Imatinib is a selective tyrosine kinase inhibitor of KIT, PDGFRA, ABL/BCR-ABL and CSF-1R, which was first used to treat GIST in 2000. Since then, it has been a standard treatment for advanced and/or recurrent GISTs.[6] Patients with advanced GIST usually respond to imatinib; however, most patients eventually experience disease progression with the reactivation of KIT tyrosine kinase and its downstream signaling pathways.[14,15] Although imatinib has high activity against GISTs, it cannot achieve complete eradication of tumor cells *in vivo* or *in vitro*. Results of the BFR14 trial showed that stopping imatinib treatment, even after complete response, resulted in disease progression or recurrence.[7,8] In chronic myelogenous leukemia (CML), mathematical models have indicated that secondary mutations might emerge after imatinib therapy;[16] therefore, residual tumor cells may also be a predisposing factor for acquired resistance to imatinib in GIST.

To quantitate the alteration of tyrosine phosphorylation levels induced by imatinib, we established quantitative tyrosine phosphoproteomic analysis. Using this technology, we identified 171 different tyrosine phosphorylation sites in 134 proteins of GIST-T1 cells. As we were searching for alternative pathways that were activated after inhibition of KIT signaling by imatinib, we pursued tyrosine kinases with increased tyrosine phosphorylation. Our comprehensive measures indicated that 11 tyrosine kinases exhibited tyrosine phosphorylation increases of greater than 1.5-fold (Table 1). The findings of the phosphoproteomic analysis were confirmed by western blotting showing the tyrosine-phosphorylation of KIT, FAK and other src-family kinases. SRC and LYN are reportedly phosphorylated and activated in GIST after imatinib treatment;[18] however, in the phosphoproteomic and western blotting analyses in the present study, we did not detect activation of SRC, LYN, YES, Lck or any other Src family kinases, except for FYN and FAK. Activation of FYN and FAK is reportedly involved in tumor proliferation and malignant transformation.[17–20]

FYN appears to participate in cell growth and survival, acting downstream of integrin and PI3K.[17,21] Although the

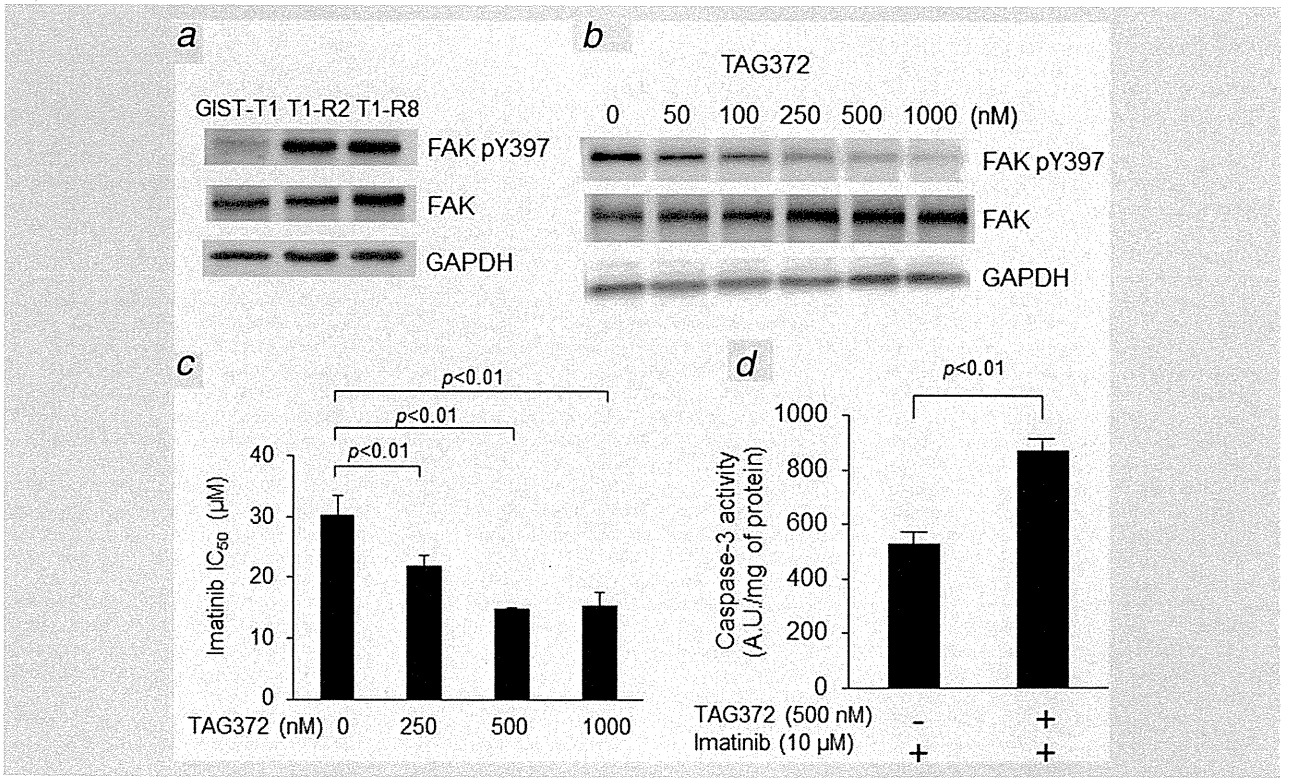

Figure 2. (*a*) Constitutive phosphorylation of FAK was observed in GIST-T1-R cells (GIST-T1-R2 and GIST-T1-R8). (*b*) Constitutive phosphorylation of FAK was observed in imatinib-resistant GIST-T1 cells (GIST-T1-R2), and TAG372 dose dependently inhibited this phosphorylation. (*c*) TAG372 reduced the IC_{50} of imatinib and induced apoptosis in GIST-T1-R2 cells. (*d*) TAG372 induced apoptosis in GIST-T1-R2 cells. Data are presented as means ± SD.

shRNA silencing of FYN induced additional cell death in GIST-T1 cells during imatinib treatment, dasatinib (a SRC family kinase inhibitor) had no effect in combination with imatinib (data not shown). These results suggest the involvement of FYN in alternative survival signaling pathways.

FAK is also a nonreceptor tyrosine kinase that is activated through autophosphorylation at Tyr^{397} by integrin and growth factor receptors; this is followed by subsequent activation of other functional phosphorylation sites to transduce the signals to downstream pathways.[22,23] FAK is reportedly overexpressed in malignant GISTs and correlated with recurrence.[19] Furthermore, FAK phosphorylation is associated with imatinib-resistance of a KIT exon 17 mutation, but not exon 11 mutation.[20] This imatinib-resistance was diminished by TAE226, which inhibits FAK and insulin-like growth factor-1 receptor. Our findings showed that imatinib induced time-dependent FAK activation in GIST-T1 cells with an imatinib-sensitive mutation of KIT exon 11. Moreover, FAK inhibition using either a FAK-specific TAG372 inhibitor or siRNA decreased the viability of GIST-T1 cells under imatinib treatment. TAG372 also induced apoptosis in imatinib-resistant cell lines with FAK activation. Taken together, it appears that FAK activation may be a critical survival signal of GIST cells under imatinib treatment, and targeting FAK with imatinib may be a promising therapeutic approach.

When imatinib was removed, KIT was quickly rephosphorylated, and FYN and FAK were simultaneously dephosphorylated (data not shown), suggesting that alternative pathway activation is functional during imatinib treatment, and may not be accompanied with qualitative changes, such as new mutations. FYN inhibition was accompanied with a subsequent lack of FAK activation, while FAK inhibition resulted in increased FYN phosphorylation, thus indicating that FYN acted upstream of FAK. However, the critical changes that induce FYN activation and subsequent FAK phosphorylation remain unknown. Additional studies are required to elucidate the FYN activation mechanisms and the alternative pathways induced by imatinib, as well as their association with acquired drug resistance.

In summary, here we found that imatinib induced increased tyrosine phosphorylation of FYN and FAK in GIST-T1 cells. Blockade of these tyrosine kinases might be a potential target to overcome imatinib resistance. Additionally, iTRAQ-based quantitative phosphotyrosine-focused proteomic analysis appears to be a useful approach to screening for phosphoproteins associated with drug resistance.

Acknowledgments

This study was partly supported by grants from Novartis Pharmaceuticals.
Conflict of interest: N.T. has honoraria to disclose from the Novatis, Pfizer and Bayer within past 2 years.

References

1. Hirota S, Isozaki K, Moriyama Y, et al. Gain-of-function mutations of c-kit in human gastrointestinal stromal tumors. *Science* 1998;279:577–80.
2. Nishida T, Hirota S, Taniguchi M, et al. Familial gastrointestinal stromal tumours with germline mutation of the kit gene. *Nat Genet* 1998;19: 323–4.
3. Hirota S, Ohashi A, Nishida T, et al. Gain-of-function mutation of platelet-derived growth factor receptor αgene in gastrtointestinal stromal tumors. *Gastroenterology* 2003;125:660–7.
4. Verweij J, Casali PG, Zalcberg J, et al. Progression-free survival in gastrointestinal stromal tumours with high-dose imatinib: randomised trial. *Lancet* 2004;364:1127–34.
5. Blanke CD, Rankin C, Demetri GD, et al. Phase III randomized, intergroup trial assessing imatinib mesylate at two dose levels in patients with unresectable or metastatic gastrointestinal stromal tumors expressing the kit receptor tyrosine kinase: S0033. *J Clin Oncol* 2008;26: 626–32.
6. Demetri GD, von Mehren M, Blanke CD, et al. Efficacy and safety of imatinib mesylate in advanced gastrointestinal stromal tumors. *N Engl J Med* 2002;347:472–80.
7. Blay JY, Le Cesne A, Ray-Coquard I, et al. Prospective multicentric randomized phase III study of imatinib in patients with advanced gastrointestinal stromal tumors comparing interruption versus continuation of treatment beyond 1 year: the French Sarcoma Group. *J Clin Oncol* 2007;25:1107–13.
8. Le Cesne A, Ray-Coquard I, Bui BN, et al. Discontinuation of imatinib in patients with advanced gastrointestinal stromal tumours after 3 years of treatment: an open-label multicentre randomised phase 3 trial. *Lancet Oncol* 2010;11: 942–9.
9. Nishida T, Shirao K, Sawaki A, et al. Efficacy and safety profile of imatinib mesylate (ST1571) in Japanese patients with advanced gastrointestinal stromal tumors: a phase II study (STI571B1202). *Int J Clin Oncol* 2008;13:244–51.
10. Mann M, Ong SE, Grønborg M, et al. Analysis of protein phosphorylation using mass spectrometry: deciphering the phosphoproteome. *Trends Biotechnol* 2002;20:261–8.
11. Rush J, Moritz A, Lee KA, et al. Immunoaffinity profiling of tyrosine phosphorylation in cancer cells. *Nat Biotechnol* 2005;23:94–101.
12. Taguchi T, Sonobe H, Toyonaga S, et al. Conventional and molecular cytogenetic characterization of a new human cell line, GIST-T1, established from gastrointestinal stromal tumor. *Lab Invest* 2002;82:663–5.
13. Yokoyama T, Enomoto T, Serada S, et al. Plasma membrane proteomics identifies bone marrow stromal antigen 2 as a potential therapeutic target in endometrial cancer. *Int J Cancer* 2013;132: 472–84.
14. Nishida T, Kanda T, Nishitani A, et al. Secondary mutations in the kinase domain of the KIT gene are predominant in imatinib-resistant gastrointestinal stromal tumor. *Cancer Sci* 2008; 99:799–804.
15. Antonescu CR, Besmer P, Guo T, et al. Acquired resistance to imatinib in gastrointestinal stromal tumor occurs through secondary gene mutation. *Clin Cancer Res* 2005;11:4182–90.
16. Michor F, Hughes TP, Iwasa Y, et al. Dynamics of chronic myeloid leukaemia. *Nature* 2005;435: 1267–70.
17. Timokhina I, Kissel H, Stella G, et al. Kit signaling through PI 3-kinase and Src kinase pathways: an essential role for Rac1 and JNK activation in mast cell proliferation. *EMBO J* 1998;17:6250–62.
18. Rossi F, Yozgat Y, de Stanchina E, et al. Imatinib upregulates compensatory integrin signaling in a mouse model of gastrointestinal stromal tumor and is more effective when combined with dasatinib. *Mol Cancer Res* 2010;8:1271–83.
19. Koon N, Schneider-Stock R, Sarlomo-Rikala M, et al. Molecular targets for tumour progression in gastrointestinal stromal tumours. *Gut* 2004;53: 235–40.
20. Sakurama K, Noma K, Takaoka M, et al. Inhibition of focal adhesion kinase as a potential therapeutic strategy for imatinib-resistant gastrointestinal stromal tumor. *Mol Cancer Ther* 2009; 8:127–34.
21. Linnekin D, DeBerry CS, Mou S. Lyn associates with the juxtamembrane region of c-Kit and is activated by stem cell factor in hematopoietic cell lines and normal progenitor cells. *J Biol Chem* 1997;272:2745–55.
22. Serrels A, McLeod K, Canel M, et al. The role of focal adhesion kinase catalytic activity on the proliferation and migration of squamous cell carcinoma cells. *Int J Cancer* 2012;131:287–97.
23. Cox BD, Natarajan M, Stettner MR, et al. New concepts regarding focal adhesion kinase promotion of cell migration and proliferation. *J Cell Biochem* 2006;99:35–52.

IJC
International Journal of Cancer

$CD34^+/CD38^-$ acute myelogenous leukemia cells aberrantly express CD82 which regulates adhesion and survival of leukemia stem cells

Chie Nishioka[1,2], Takayuki Ikezoe[3], Mutsuo Furihata[4], Jing Yang[3], Satoshi Serada[5], Tetsuji Naka[5], Atsuya Nobumoto[6], Sayo Kataoka[7], Masayuki Tsuda[6], Keiko Udaka[1] and Akihito Yokoyama[3]

[1] Department of Immunology, Kochi Medical School, Kochi University, Nankoku, Kochi, Japan
[2] Japanese Society for the Promotion of Science (JSPS), Chiyoda-ku, Tokyo, Japan
[3] Hematology and Respiratory Medicine, Kochi Medical School, Kochi University, Nankoku, Kochi, Japan
[4] Tumor Pathology, Kochi Medical School, Kochi University, Nankoku, Kochi, Japan
[5] Laboratory for immune Signal, National Institute of Biomedical Innovation, Ibaraki, Osaka
[6] The Facility for Animal Research, Kochi Medical School, Kochi University, Nankoku, Kochi, Japan
[7] Medical Research Center, Kochi Medical School, Kochi University, Nankoku, Kochi, Japan

Cancer Cell Biology

To identify molecular targets in leukemia stem cells (LSCs), this study compared the protein expression profile of freshly isolated $CD34^+/CD38^-$ cells with that of $CD34^+/CD38^+$ counterparts from individuals with acute myelogenous leukemia (n = 2, AML) using isobaric tags for relative and absolute quantitation (iTRAQ). A total of 98 proteins were overexpressed, while six proteins were underexpressed in $CD34^+/CD38^-$ AML cells compared with their $CD34^+/CD38^+$ counterparts. Proteins overexpressed in $CD34^+/CD38^-$ AML cells included a number of proteins involved in DNA repair, cell cycle arrest, gland differentiation, antiapoptosis, adhesion, and drug resistance. Aberrant expression of CD82, a family of adhesion molecules, in $CD34^+/CD38^-$ AML cells was noted in additional clinical samples (n = 12) by flow cytometry. Importantly, down-regulation of CD82 in $CD34^+/CD38^-$ AML cells by a short hairpin RNA (shRNA) inhibited adhesion to fibronectin *via* up-regulation of matrix metalloproteinases 9 (MMP9) and colony forming ability of these cells as assessed by transwell assay, real-time RT-PCR, and colony forming assay, respectively. Moreover, we found that down-regulation of CD82 in $CD34^+/CD38^-$ AML cells by an shRNA significantly impaired engraftment of these cells in severely immunocompromised mice. Taken together, aberrant expression of CD82 might play a role in adhesion of LSCs to bone marrow microenvironment and survival of LSCs. CD82 could be an attractive molecular target to eradicate LSCs.

Key words: AML, leukemia stem cells, bone marrow microenvironment, CD82, MMP9
Additional Supporting Information may be found in the online version of this article.
*Takayuki Ikezoe contributed to the concept and design, interpreted and analyzed the data and wrote an article. Chie Nishioka performed all experiments and wrote an article. Mutsuo Furihata, Jing Yang, Satoshi Serada, and Tetsuji Naka, Sayo Kataoka and Atsuya Nobumoto performed the experiments. Akihito Yokoyama and Keiko Udaka provided important intellectual content
Grant sponsors: The Kochi University President's Discretionary Grant, Setsuro Fujii Memorial, The Osaka Foundation for Promotion of Fundamental Medical Research, Certificate of Kochi Shin-kin/Anshin-tomo-no-kai Prize and Japan Society for the Promotion of Science
DOI: 10.1002/ijc.27904
History: Received 15 Mar 2012; Accepted 25 Sep 2012; Online 11 Oct 2012
Correspondence to: Takayuki Ikezoe, Department of Hematology and Respiratory Medicine, Kochi University, Oko-cho, Nankoku, Kochi 783-8505, Japan, Tel.: 81-88-880-2345, Fax: 81-88-880-2348, E-mail: ikezoet@kochi-u.ac.jp

Acute myelogenous leukemia (AML) is characterized by a cellular hierarchy, and is initiated and maintained by a subset of self-renewing leukemia stem cells (LSCs).[1] To produce cure in individuals with AML, development of a novel treatment strategy targeting LSCs is urgently required. LSCs share some antigenic features with normal hematopoietic stem cells (HSCs). For example, both LSCs and HSCs express CD34 but not CD38. However, LSCs can be phenotypically distinguished from HSCs by several disparate markers, including $CD117^-$ and $CD123^+$.[1–3] LSCs exist in a quiescent state and are capable of self-renewal and differentiation, and are able to perpetuate leukemic cell growth in long-term culture assays and in the murine nonobese diabetic/severe combined immunodeficiency (NOD/SCID) model system.[1–4] $CD34^+/CD38^-$ AML cells were shown to fulfill the criteria for LSCs *in vivo*.[5,6] Although, recent studies employed more severely immunocompromised mice found that even $CD34^-$ or $CD38^+$ AML cells in some cases were able to reconstitute AML.[7,8]

The regulation of stem cell self-renewal and differentiation requires a specific microenvironment of surrounding cells known as the stem cell niche. The concept of the stem cell niche was first proposed for the human hematopoietic system in the 1970s.[9] The HSC niche in mouse bone marrow (BM) is

What's new?
Acute myelogenous leukemia (AML) is maintained by a subset of self-renewing leukemia stem cells (LSCs). Thus, to effectively treat AML, treatments targeting LSCs are needed. AML cells expressing CD34 but not CD38 (CD34+/CD38-) contain abundant LSCs and were found in this study to express a greater amount of CD82 than CD34+/CD38+ AML cells. CD82 was further found to regulate the survival of CD34+/CD38- AML cells and their adhesion to the bone marrow microenvironment, suggesting that this glycoprotein could be an attractive target for LSC eradication.

composed of an endosteal lining of stromal cells, extracellular matrix proteins, and osteoblasts.[10–12] Specific adherens junction molecules such as N-cadherin mediate adhesion between HSCs and niche cells in the adult hematopoietic system.[11]

Recent work has shown that interaction between CXCR4 on leukemic cells and its ligand stromal cell-derived factor-1 (SDF-1) in the niche is necessary for proper homing and *in vivo* growth of leukemic cells.[13] Moreover, interaction between LSCs and the niche mediated by adhesion molecule CD44 is required for maintenance of LSCs behavior.[14] CD44 mediates adhesive cell-cell and cell-extracellular matrix interactions by binding its main ligand, hyaluronan, a glycosaminoglycan that is highly concentrated in the endosteal region.[14,15] All together, adhesion molecules play an important role in maintaining the characteristics of LSCs.

CD82/KAI-1, a member of the tetraspanin superfamily, was originally identified as an accessory molecule in T-cell activation.[16] The most well-characterized function of CD82 in nonimmune cells is integrin-mediated cell adhesion to extracellular matrix.[17] Forced expression of CD82 up-regulated tissue inhibitors of metalloproteinase 1 (TIMP1) and inactivated matrix metalloproteinases 9 (MMP9) in the H1299 human lung carcinoma cells, resulting in suppression of tumor invasion and metastasis.[18] Cell adhesion to collagen I, which is one of the major proteins in the bone marrow (BM) niche, is mostly mediated by three integrin receptors $\alpha1\beta1$, $\alpha2\beta1$, and $\alpha11\beta1$ expressed on cell surface of mesenchymal stem cells.[19] Integrin may associate with CD82 in $CD34^+/CD38^-$ AML cells to promote adhesion to the endosteal niche. However, the roles of CD82 in hematopoietic cells remain to be elucidated.

In this study, we analyzed the protein expression profile of freshly isolated $CD34^+/CD38^-$ AML cells from individuals with AML and compared it with the expression profile of their $CD34^+/CD38^+$ counterparts using isobaric tags for relative and absolute quantitation (iTRAQ) and found the aberrant expression of CD82 in $CD34^+/CD38^-$ AML cells. This study also explored the function of CD82 in $CD34^+/CD38^-$ AML cells *in vitro* as well as *in vivo* by utilizing NOD.Cg-*Rag1*^{tm1Mom} *Il2rg*^{tm1Wjl}/SzJ mice.

Material and Methods

Sample collection and isolation of $CD34^+/CD38^-$ AML cells and their $CD34^+/CD38^+$ counterparts

Leukemia cells were freshly isolated from AML patients (n = 18) with World Health Organization (WHO) classification system subtype minimally differentiated AML (case 6), AML without maturation (cases 1 and 10), AML with maturation (cases 2, 7, and 12), acute myelomonocytic leukemia (cases 4, 14, and 15), AML with myelodysplasia changes (cases 3, 5, 8, 9,16, 17, and 18), and therapy-related AML (cases 11 and 13) after obtaining informed consent with Kochi University Institutional Review Board approval (Supporting Information Table S1). The informed consent was obtained in accordance with the Declaration of Helsinki. $CD34^+/CD38^-$ AML cells and $CD34^+/CD38^+$ counterparts were purified by magnetic cell sorting utilizing a CD34 MultiSort kit and a CD38 MicroBead kit (Miltenyi Biotec GmbH, Germany), as previously described (Supporting Information Fig. S1*a*).[20]

Cells

Chronic eosinophilic leukemia (CEL) EOL-1 cells were obtained from RIKEN BRC Cell Bank (Tsukuba, Japan). Imatinib-resistant EOL-1R cell line was established by culturing with increasing concentrations of imatinib (from 1 to 100 nM) for 6 months.[21] Most of EOL-1R cells expressed CD34 (92 ± 9%) on their cell surface. On the other hand, CD34 was rarely detectable on cell surface of parental EOL-1 cells (0.1 ± 0.1%) (figure not shown).

Isolation and culture of primary mesenchymal stromal cells (MSCs)

MSCs were isolated from a BM of healthy donors. BM cells were subjected to centrifugation over a Ficoll-Hypaque gradient to separate mononuclear cells. These cells were resuspended in α-minimal essential medium (Gibco BRL, Rockville, MD) containing 20% fetal bovine serum (FBS) and plated at an initial density of 10^6 cells.[22]

Protein extraction

Proteins were extracted using the complete mammalian proteome kit (539779, Calbiochem, Darmstadt, Germany), according to the manufacturer's instructions.

iTRAQ labeling of peptides

Each protein sample (100 μg) was digested with trypsin and labeled with iTRAQ reagents (Applied Biosystems, Framingham, MA) according to the manufacturer's instructions. Briefly, the proteins extracted from $CD34^+/CD38^-$ AML cells were labeled with iTRAQ reagents 114 (case 1) or 116 (case 2), and proteins extracted from $CD34^+/CD38^+$ counterparts

Table 1. PCR primers

Gene	Direction	Primer
MMP9	Forward	5′-CTCGAACTTTGACAGCGACA-3′
	Reverse	5′-GCCATTCACGTCGTCCTTAT-3′
MMP2	Forward	5′-ACCCAGATGTGGCCAACTAC-3′
	Reverse	5′-TCATGATGTCTGCCTCTCCA-3′
18S	Forward	5′-AAACGGCTACCACATCCAAG-3′
	Reverse	5′-CCTCCAATGGATCCTCGTTA-3′

were labeled with iTRAQ reagents 115 (case 1) or 117 (case 2). Labeled peptide samples were mixed and fractionated as described previously.[23]

Mass spectrometric analysis

NanoLC-MS/MS analyses were performed on an LTQ-Orbitrap XL (Thermo Fisher Scientific, Waltham, MA) equipped with a nano-ESI source and coupled to a Paradigm MG2 pump (Michrom Bioresources, Auburn, CA) and autosampler (HTC PAL, CTC Analytics, Zwingen, Switzerland).[23]

iTRAQ data analysis

Protein identification and quantitation for iTRAQ analysis was carried out using SEQUEST (Bioworks version 3.3.1, Thermo Fisher Scientific) searching against the International Protein Index (IPI) human protein database (version 3.26).[23] Relative protein abundances were determined by comparing the ratio of iTRAQ reporter ion intensities in the MS/MS scan.[23]

Quantitation of CD82-expressing cells using flow cytometry (FACS)

Leukemic peripheral blood (PB) ($n = 3$) and BM ($n = 9$) cells were collected from 12 AML patients (case numbers 1–12) after obtaining informed consent. Leukemic cells were stained with a fluorescein isothiocyanate (FITC)-conjugated monoclonal antibody (mAb) against CD34 (Beckman coulter, CA), a phycoerythrin (PE)-conjugated mAb against CD82 (Abcam, Cambridge, UK), and a PE Cy5-conjugated mAb against CD38 (BioLegend, San Jose, CA). Cells were stained for 30 min on ice. Isotypo-matched immunoglobulins were used as controls. Cells were then analyzed using flow cytometry (FACS Calibur, Becton Dickinson, San Jose, CA) following data analysis by FlowJo software (TreeStar, San Carlos, CA).

RNA isolation and real-time reverse transcription-polymerase chain reaction (RT-PCR)

RNA isolation and cDNA preparation were performed as described previously.[24] Real-time RT-PCR was carried out by using Power SYBR Green PCR Master Mix (Applied Biosystems, Warrington, UK) as described previously.[24] Primers for PCR are shown in Table 1.

Small interfering RNA

Control small interfering (si) RNA and an siRNA against CD82 were purchased from Santa Cruz Biotechnology and Sigma (Deisenhofen, Germany), respectively.

Transfections

EOL-1 and EOL-1R cells were transiently transfected with either control or CD82 siRNA (300 nM) using an Amaxa Nucleofector II electroporator (Wako Pure Chemical Industries, Ltd., Osaka, Japan) with a Nucleofector Kit V (program U-001) as previously described.[25] The preliminary experiments using the green fluorescence protein-expressing vector found that efficacy of transfection with this program was approximately 70% with nearly 70% cell viability, as measured by FACS and Annexin V/PI staining, respectively (figure not shown).

CD82 shRNA lentiviral vector, production and infection

The short hairpin (sh) RNA sequence used to target human CD82 corresponded to the following sequence on the human CD82 transcript variant 2, NCB I accession number NM_001024844. Lentiviral shRNA particles were produced using the viral power packaging system (Invitrogen, CA) with the 293FT packaging cell line (Invitrogen), and lentiviral CD82 shRNA particles (>10^8 titer unit (TU)/ml) were prepared using ultracentrifugation. 5×10^4 $CD34^+/CD38^-$ AML cells were seeded in 24-well plates in 500 μl of Iscove's modified Dulbecco's medium (IMDM) (Invitrogen) containing 10% heat inactivated fetal bovine serum (FBS). After overnight incubation, 5×10^5 TU lentiviral CD82 shRNA particles and polybrene (10 μg/ml) were added per well with serum free medium containing IMDM. After overnight, 1 ml of full media supplemented with FBS, 2-mercaptoethanol, stem cell factor, granulocyte-macrophage colony-stimulating factor (GM-CSF), granulocyte-colony-stimulating factor (G-CSF), IL-3, and erythropoietin (EPO) was added and incubated for 7 days. The control and CD82 shRNA lentiviral vectors co-expressed green fluorescence protein (GFP). Quantification of GFP-positive cells using FACS analysis indicated that the lentiviral transduction efficiency was nearly 70% (Supporting Information Fig. S1*b*). GFP-positive cells were sorted using JSAN (Bay bioscience Co., Ltd., Kobe, Japan).

CD82 lentiviral vector

CD82 cDNA was purchased from Mammalian gene collection (BC000726) and was used as the template for PCR. PCR products were cloned into pLenti6.3/V5-TOPO vector (Invitrogen). CD82-transfected lentiviral particles were produced using the viral power packaging system (Invitrogen) with the 293FT packaging cell line (Invitrogen). The pLenti6.3/V5-TOPO vector was designed to co-express V5 epitope; 5×10^4 $CD34^+/CD38^+$ AML cells were seeded in 24-well plates in 500 μl of IMDM (Invitrogen) containing 10% FBS. After overnight incubation, 5×10^5 TU lentiviral CD82-transfected